

Accessible quantification of multiparticle entanglement

Marco Cianciaruso,^{1,2,3,*} Thomas R. Bromley,^{1,†} and Gerardo Adesso^{1,‡}

¹School of Mathematical Sciences, The University of Nottingham,
University Park, Nottingham NG7 2RD, United Kingdom

²Dipartimento di Fisica “E. R. Caianiello”, Università degli Studi di Salerno, Via Giovanni Paolo II, I-84084 Fisciano (SA), Italy

³INFN, Sezione di Napoli, Gruppo Collegato di Salerno, I-84084 Fisciano (SA), Italy

Entanglement is a key ingredient for quantum technologies and a fundamental signature of quantumness in a broad range of phenomena encompassing many-body physics, thermodynamics, cosmology, and life sciences. For arbitrary multiparticle systems, entanglement quantification typically involves nontrivial optimisation problems, and may require demanding tomographical techniques. Here we develop an experimentally feasible approach to the evaluation of geometric measures of multiparticle entanglement. Our approach provides analytical results for particular classes of mixed states of N qubits, and computable lower bounds to global, partial, or genuine multiparticle entanglement of any general state. For global and partial entanglement, useful bounds are obtained with minimum effort, requiring local measurements in just three settings for any N . For genuine entanglement, a number of measurements scaling linearly with N is required. We demonstrate the power of our approach to estimate and quantify different types of multiparticle entanglement in a variety of N -qubit states useful for quantum information processing and recently engineered in laboratories with quantum optics and trapped ion setups.

I. INTRODUCTION

The fascination with quantum entanglement has evolved over the last eight decades, from the realm of philosophical debate [1] to a very concrete recognition of its resource role in a range of applied sciences [2]. While considerable progress has been achieved in the detection of entanglement [3], its full *quantification* in general states is almost always unfeasible [4, 5]. Quantifying entanglement is yet necessary to gauge precisely the quantum enhancement in information processing and computation [2], and to pin down exactly how much a physical or biological system under observation departs from an essentially classical behaviour [6]. This is especially relevant in the case of complex, multiparticle systems, for which only quite recently have notable advances been reported both on the experimental control [7–10] as well as on the theoretical classification [11–16] and, in very few cases, quantification [17–23] of specific forms of entanglement.

An intuitive framework for classifying and quantifying the degree of multiparticle entanglement relies on a geometric perspective [24–26]. Within this approach, one first identifies a hierarchy of non-entangled multiparticle states, also referred to as M -separable states for $2 \leq M \leq N$, where N is the number of particles composing the quantum system of interest; see Figure 1. Introducing then a distance functional D respecting natural properties of contractivity under quantum operations and joint convexity (see Methods) [27], the quantity E_M^D defined as

$$E_M^D(\varrho) = \inf_{\varsigma \text{ } M\text{-separable}} D(\varrho, \varsigma), \quad (1)$$

is a valid geometric measure of (M -inseparable) *multiparticle entanglement* in the state ϱ .

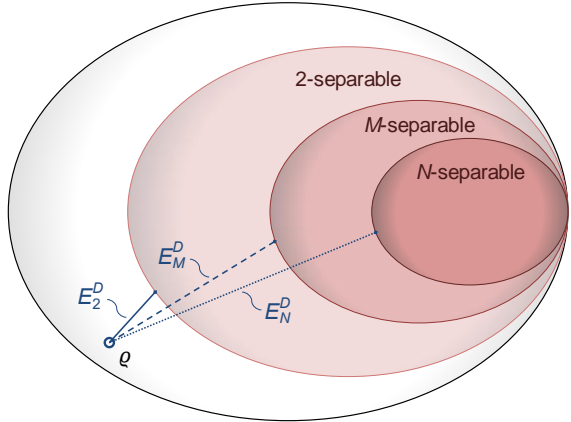


FIG. 1. Geometric picture of multiparticle entanglement in a quantum system of N particles. Each red-shaded convex set contains M -separable states (for $2 \leq M \leq N$), which can be defined as follows. The set of pure M -separable states is given by the union of the sets of tensor products $|\Psi_M\rangle = \bigotimes_{k=1}^M |\psi^{(k)}\rangle$ of pure states $|\psi^{(k)}\rangle$, with respect to any partition of the N particles into M subsystems $k = 1, \dots, M$; the set of general (mixed) M -separable states is then formed by all convex mixtures of pure M -separable states, where each term in the mixture may be factorised with respect to a different multipartition. This provides a partition-independent classification of separability (see also the Supplementary Material). For any M , the multiparticle entanglement measure E_M^D of a state ϱ is defined as the minimum distance, with respect to a contractive and jointly convex distance functional D , from the set of M -separable states. We refer to the case $M = N$ (dotted line) as global entanglement, the case $M = 2$ (solid line) as genuine entanglement, and any intermediate case (dashed line) as partial entanglement, as detailed in the main text.

Some special cases are prominent in this hierarchy. For $M = N$, the distance from N -separable (also known as fully separable) states defines the *global* multiparticle entanglement E_N^D , which accounts for any form of entanglement distributed among two or more of the N particles. Geometric measures

* cianciaruso.marco@gmail.com

† thomas.r.bromley@gmail.com

‡ gerardo.adesso@nottingham.ac.uk

of global entanglement have been successfully employed to characterise quantum phase transitions in many-body systems [28] and directly assess the usefulness of initial states for Grover's search algorithms [29]. On the other extreme of the hierarchy, for $M = 2$, the distance from 2-separable (also known as biseparable) states defines instead the *genuine* multiparticle entanglement E_2^D , which quantifies the entanglement shared by all the N particles, that is the highest degree of inseparability. Genuine multiparticle entanglement is an essential ingredient for quantum technologies including multiuser quantum cryptography [30], quantum metrology [31], and measurement-based quantum computation [32]. Finally, for any intermediate M , we can refer to E_M^D as *partial* multiparticle entanglement. The presence of partial entanglement is relevant in quantum informational tasks such as quantum secret sharing [33] and may play a relevant role in biological phenomena [6, 34]. Probing and quantifying different types of entanglement can shed light on which nonclassical features of a mixed multiparticle state are necessary for quantum-enhanced performance in specific tasks [14] and can guide the understanding of the emergence of classicality in multiparticle quantum systems of increasing complexity [35].

The quantitative amount of multiparticle entanglement, be it global or genuine (or any intermediate type), has an intuitive operational meaning when adopting the geometric approach. Namely, E_M^D measures how distinguishable a given state ϱ is from the closest M -separable state. Given some widely adopted metrics, such a distinguishability is directly connected to the usefulness of ϱ for quantum information protocols relying on multiparticle entanglement. For instance, the trace distance of entanglement is operationally related to the minimum probability of error in the discrimination between ϱ and any M -separable state with a single measurement [27]. Furthermore, the geometric entanglement with respect to relative entropy or Bures distance sets quantitative bounds on the number of orthogonal states that can be discriminated by local operations and classical communication [36]. The geometric entanglement based on infidelity [25] (monotonically related to Bures distance) has also a dual interpretation based on the convex roof construction [37], that is, it quantifies the minimum price (in units of pure-state entanglement) that has to be spent on average to create a given density matrix ϱ as a statistical mixture of pure states.

It is therefore clear that finding the minimum in Eq. (1), hence evaluating geometric measures of multiparticle entanglement defined by meaningful distances on practically relevant states, is a central challenge to benchmark quantum technologies. Mathematically, however, this is in principle a formidable problem.

Here we provide substantial advances towards addressing this problem. We focus initially on a family of mixed states ϖ of N qubits, that we label \mathcal{M}_N^3 states, which form a particular subset of the class of states having all maximally mixed marginals. This family includes maximally entangled Bell states of two qubits and their mixtures, as well as multiparticle bound entangled states [38–41]. For any N , these states are completely specified by three easily measurable quantities, given by the correlation functions $c_j = \langle \sigma_j^{\otimes N} \rangle$, where

$\{\sigma_j\}_{j=1,2,3}$ are the Pauli matrices. In the following we show how every entanglement monotone E_M^D can be evaluated exactly for any even N on these states, by revealing an intuitive geometric picture common to all valid distances D . For odd N , the results are distance-dependent; we show nonetheless that E_M^D can still be evaluated exactly if D denotes the trace distance. The results are nontrivial for all $M > \lceil N/2 \rceil$ in the hierarchy of Figure 1. A central observation is that an arbitrary state of N qubits can be transformed into an \mathcal{M}_N^3 state by local operations and classical communication, which cannot increase entanglement by definition. This implies that our exact formulae readily provide practical lower bounds to the degree of global and partial multiparticle entanglement in completely general states. Importantly, the bounds are obtained by measuring only the three correlation functions $\{c_j\}$ for any number of qubits, and can be further improved by adjusting the local measurement basis (see Figure 2 for an illustration).

We then discuss how our analysis can be extended to allow for the identification and quantitative estimation of genuine multiparticle entanglement as well, at the cost of performing extra measurements. Since \mathcal{M}_N^3 states are always biseparable, a different reference set is needed for such a study. We focus on the class of N -qubit states obtained as mixtures of Greenberger-Horne-Zeilinger (GHZ) states [11, 42], the latter being central resources for quantum communication and estimation; this class of states depends on $2^N - 1$ real parameters. We calculate exactly distance-based measures of genuine multiparticle entanglement E_2^D for these states, for every valid D . Once more, these analytical results provide lower bounds to geometric measures of genuine entanglement for any general state of N qubits, obtainable experimentally in this case by performing at least $N + 1$ local measurements [43].

We demonstrate that our methods provide overall accessible quantitative assessments of global, partial, and genuine multiparticle entanglement in a variety of noisy states produced in recent experiments [35, 39, 44–47], going beyond the mere detection obtainable by entanglement witnesses [3, 43, 48–51], yet with no added experimental overhead. Compared with some recent complementary approaches to the characterisation of multiparticle entanglement [17, 19, 20, 23], we find that our approach fares surprisingly well in its efficiency and versatility despite the minimal experimental requirements.

II. RESULTS

A. Global and partial multiparticle entanglement

We define an \mathcal{M}_N^3 state as $\varpi = \frac{1}{2^N} \left(\mathbb{I}^{\otimes N} + \sum_{j=1}^3 c_j \sigma_j^{\otimes N} \right)$, where \mathbb{I} is the 2×2 identity matrix. These states are invariant under permutations of any pair of qubits and enjoy a nice geometrical representation in the space of the three correlation functions c_j , corresponding to a tetrahedron for even N and to the unit ball for odd N , as depicted in Figure 2. We can then characterise the subset of M -separable \mathcal{M}_N^3 states for any N . We find that, if $M > \lceil N/2 \rceil$, then the M -separable \mathcal{M}_N^3 states fill a subset corresponding to an octahedron in the space of the correlation functions (see Figure 2). When $M \leq \lceil N/2 \rceil$, all

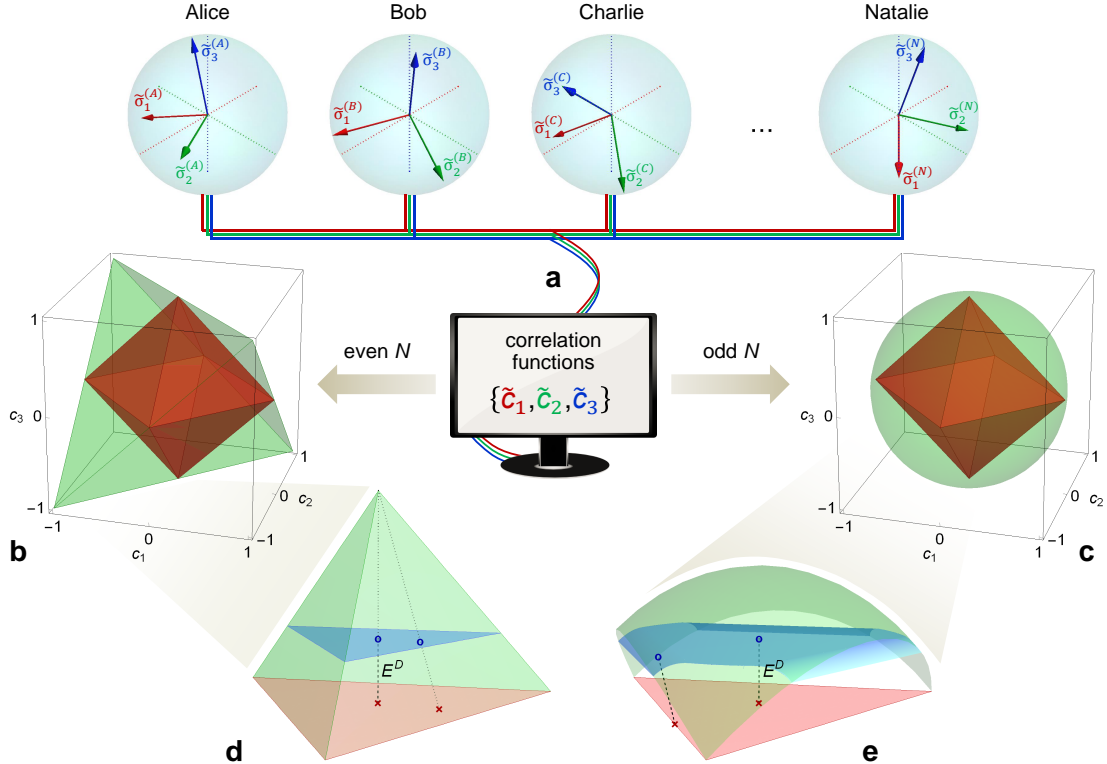


FIG. 2. Experimentally friendly approach to quantify global and partial N -particle entanglement. *Top row*: (a) A state ρ of N qubits is shared by N parties, named Alice, Bob, Charlie, ..., Natalie. Each party, labelled by $\alpha = A, \dots, N$, locally measures her or his qubit in three orthogonal directions $\{\tilde{\sigma}_j^{(\alpha)}\}$, with $j = 1, 2, 3$, indicated by the solid arrows. If the shared state ρ is completely unknown, a standard choice can be to measure the three canonical Pauli operators for all the qubits (corresponding to the directions of the dashed axes); if instead some partial information on ρ is available, the measurement directions can be optimised a priori. Once all the data are collected, the N parties communicate classically to construct the three correlation functions $\{\tilde{c}_j\}$, with $\tilde{c}_j = \langle \bigotimes_{\alpha} \tilde{\sigma}_j^{(\alpha)} \rangle$. *Middle row*: For any N , one can define a reference subset of N -qubit states with all maximally mixed marginals (M_N^3 states), which are completely specified by a triple of orthogonal correlation functions $\{c_j\}$. These states enjoy a convenient representation in the space of $\{c_1, c_2, c_3\}$. (b) For even N , M_N^3 states fill the tetrahedron with vertices $\{1, (-1)^{N/2}, 1\}$, $\{-1, (-1)^{N/2}, 1\}$, $\{1, -(-1)^{N/2}, -1\}$ and $\{-1, -(-1)^{N/2}, -1\}$. (c) For odd N , they are instead contained in the unit Bloch ball. For any $M > \lceil N/2 \rceil$, M -separable M_N^3 states are confined to the octahedron with vertices $\{\pm 1, 0, 0\}$, $\{0, \pm 1, 0\}$ and $\{0, 0, \pm 1\}$, illustrated in red in both panels; conversely, for $M \leq \lceil N/2 \rceil$, all M_N^3 states are M -separable. *Bottom row*: Geometric analysis of multiparticle entanglement. The bottom panels depict zooms of (d) a corner of the tetrahedron for even N and (e) a sector of the unit sphere for odd N , opposing a face of the octahedron of M -separable M_N^3 states (for $M > \lceil N/2 \rceil$). Instances of inseparable M_N^3 states are indicated by blue circles, and their closest M -separable states by red crosses. The cyan surfaces in each of the two bottom panels contain states with equal global and partial multiparticle entanglement E_M^D , which we compute exactly. The results are valid for any contractive and jointly convex distance D in the even N case, and for the trace distance in the odd N case. The entanglement of an M_N^3 state with correlation functions $\{\tilde{c}_1, \tilde{c}_2, \tilde{c}_3\}$ provides an analytical lower bound for the entanglement of any N -qubit state with the same correlation functions, such as the state ρ initially shared by the N parties in (a). The bound is effective for the most relevant families of N -qubit states in theoretical and experimental investigations of quantum information processing, as we show in the article.

M_N^3 states are instead M -separable. The proofs are deferred to the Supplementary Material.

We can now tackle the quantification of global and partial multiparticle entanglement in these states; for the latter, we will always focus on the nontrivial case $M > \lceil N/2 \rceil$ throughout this section. First, we observe that the closest M -separable state ς_{ϖ} to an M_N^3 state ϖ , which solves the optimisation in Eq. (1), can always be found within the subset of M -separable M_N^3 states, yielding a considerable simplification of the general problem. To find the exact form of ς_{ϖ} , and consequently of $E_M^D(\varpi)$, we approach the cases of even and odd N separately.

For even N , we prove that there exists a unique solution to the minimisation in Eq. (1), independent of the specific choice of contractive and jointly convex distance D . Namely, the closest M -separable state ς_{ϖ} is on the face of the octahedron bounding the corner of the tetrahedron in which ϖ is located, and is identified by the intersection of such octahedron face with the line connecting ϖ to the vertex of the tetrahedron corner, as depicted in Figure 2(d). It follows that, for any nontrivial M , valid D , and even N , the multiparticle entanglement $E_M^D(\varpi^{[c_j]})$ of an M_N^3 state $\varpi^{[c_j]}$ with correlation functions $\{c_j\}$ is only a monotonically increasing function of the Euclidean distance between the point of coordinates $\{c_j\}$ and

the closest octahedron face, which is in turn proportional to $h_{\varpi} = \frac{1}{2}(\sum_{j=1}^3 |c_j| - 1)$ (notice that h_{ϖ} equals the bipartite measure known as concurrence for $N = 2$ [4, 52]). We have then a closed formula for any valid geometric measure of global and partial multiparticle entanglement on an arbitrary \mathcal{M}_N^3 state $\varpi^{\{c_j\}}$ with even N , given by

$$E_M^D(\varpi^{\{c_j\}}) = \begin{cases} 0, & h_{\varpi} \leq 0 \text{ (or } M \leq N/2\text{)}; \\ f_D(h_{\varpi}), & \text{otherwise,} \end{cases} \quad (2)$$

where f_D denotes a monotonically increasing function whose explicit form is specific to each distance D . In Table I we present the expression of f_D for relevant distances in quantum information theory.

Distance D	$D(\varrho, \varsigma)$	$f_D(h_{\varpi})$
Relative entropy D_{RE}	$\text{Tr}[\varrho(\log_2 \varrho - \log_2 \varsigma)]$	$\frac{1}{2}[(1 - h_{\varpi})\log_2(1 - h_{\varpi}) + (1 + h_{\varpi})\log_2(1 + h_{\varpi})]$
Trace D_{Tr}	$\frac{1}{2}\text{Tr} \varrho - \varsigma $	$\frac{1}{2}h_{\varpi}$
Infidelity D_F	$1 - \left[\text{Tr}\left(\sqrt{\varsigma\varrho}\sqrt{\varsigma}\right)\right]^2$	$\frac{1}{2}(1 - \sqrt{1 - h_{\varpi}^2})$
Squared Bures D_B	$2\left[1 - \text{Tr}\left(\sqrt{\varsigma\varrho}\sqrt{\varsigma}\right)\right]$	$2 - \sqrt{1 - h_{\varpi}} - \sqrt{1 + h_{\varpi}}$
Squared Hellinger D_H	$2\left[1 - \text{Tr}\left(\sqrt{\varrho}\sqrt{\varsigma}\right)\right]$	$2 - \sqrt{1 - h_{\varpi}} - \sqrt{1 + h_{\varpi}}$

TABLE I. Analytical expression of global and partial multiparticle entanglement E_M^D for \mathcal{M}_N^3 states of an even number N of qubits as defined by Eq. (2), for representative choices of the distance D .

For odd N , the closest M -separable state ς_{ϖ} to any \mathcal{M}_N^3 state ϖ is still independent of (any nontrivial) M . However, different choices of D in Eq. (1) are minimised by different states ς_{ϖ} . We focus on the important but notoriously hard-to-evaluate case of the trace distance $D_{\text{Tr}}(\varpi, \varsigma)$ (see Table I). In the representation of Figure 2(c), the trace distance amounts to half the Euclidean distance on the unit ball. It follows that the closest M -separable state ς_{ϖ} to ϖ is the Euclidean orthogonal projection onto the boundary of the octahedron, see Figure 2(e). We can then get a closed formula for the trace distance measure of global and partial multiparticle entanglement $E_M^{D_{\text{Tr}}}(\varpi^{\{c_j\}})$ of an arbitrary \mathcal{M}_N^3 state $\varpi^{\{c_j\}}$ with odd N as well, given by

$$E_M^{D_{\text{Tr}}}(\varpi^{\{c_j\}}) = \begin{cases} 0, & h_{\varpi} \leq 0 \text{ (or } M \leq \lceil N/2 \rceil\text{)}; \\ \frac{h_{\varpi}}{\sqrt{3}}, & 0 < h_{\varpi} \leq 3|c_j|/2 \forall j; \\ \min_j \frac{1}{2}\sqrt{|c_j|^2 + \frac{1}{2}(2h_{\varpi} - |c_j|)^2}, & \text{otherwise.} \end{cases} \quad (3)$$

The usefulness of the just derived analytical results for multiparticle entanglement is not limited to the \mathcal{M}_N^3 states. A crucial observation is that the \mathcal{M}_N^3 states are *extremal* among all quantum states with given correlation functions $\{c_j\}$. Specifically, any general state ϱ of N qubits can be transformed into an \mathcal{M}_N^3 state with the same $\{c_j\}$ by means of a procedure that we name \mathcal{M}_N^3 -fication, involving only local operations and classical communication (see Methods). This immediately

implies that, for any $M > \lceil N/2 \rceil$, the multiparticle entanglement E_M^D of ϱ can have a nontrivial exact lower bound given by the corresponding multiparticle entanglement of the \mathcal{M}_N^3 state ϖ with the same $\{c_j\}$,

$$E_M^D(\varpi^{\{c_j\}}) \leq E_M^D(\varrho), \forall \varrho : \text{Tr}(\varrho \sigma_j^{\otimes N}) = c_j (j = 1, 2, 3). \quad (4)$$

From a practical point of view, one needs only to measure the three correlation functions $\{c_j\}$, as routinely done in optical, atomic, and spin systems [3, 39, 44, 45], to obtain an estimate of the global and partial multiparticle entanglement content of an unknown state ϱ with no need for a full state reconstruction.

Furthermore, the lower bound can be improved if a partial knowledge of the state ϱ is assumed, as is usually the case for experiments aiming to produce specific families of states for applications in quantum information processing [39, 40, 44]. In those realisations, one typically aims to detect entanglement by constructing optimised entanglement witnesses tailored on the target states [3]. By exploiting similar ideas, we can optimise the quantitative lower bound in Eq. (4) over all possible single-qubit local unitaries applied to the state ϱ before the \mathcal{M}_N^3 -fication,

$$\sup_{U_{\otimes}} E_M^D(\varpi^{\{\tilde{c}_j\}}) \leq E_M^D(U_{\otimes} \varrho U_{\otimes}^{\dagger}) = E_M^D(\varrho), \quad (5)$$

where $\text{Tr}(U_{\otimes} \varrho U_{\otimes}^{\dagger} \sigma_j^{\otimes N}) = \tilde{c}_j$ and $U_{\otimes} = \bigotimes_{a=1}^N U^{(a)}$ denotes a single-qubit local unitary operation. Experimentally, the optimised bound can then be still accessed by measuring a triple of correlations functions $\{\tilde{c}_j\}$ given by the expectation values of correspondingly rotated Pauli operators on each qubit, $\tilde{c}_j = \langle U_{\otimes}^{\dagger} \sigma_j^{\otimes N} U_{\otimes} \rangle$, as illustrated in Figure 2(a). Optimality in Eq. (5) can be achieved by the choice of U_{\otimes} such that $\tilde{h}_{\varpi} = \frac{1}{2}(\sum_{j=1}^3 |\tilde{c}_j| - 1)$ is maximum. The optimisation procedure can be significantly simplified when considering a state ϱ which is invariant under permutations of any pair of qubits. In such a case, one may need to optimise only over three angles $\{\theta, \psi, \phi\}$ parameterising a generic unitary applied to each single qubit; the optimisation can be equivalently performed over an orthogonal matrix acting on the Bloch vector of each qubit (see Methods).

We can now investigate how useful our approach is on concrete examples. Table II presents a compendium of optimised analytical lower bounds on the global and partial multiparticle entanglement of several relevant families of N -qubit states [41, 42, 46, 47, 53–57, 61–63], up to $N = 8$. All the bounds are experimentally accessible by measuring the three correlation functions $\{\tilde{c}_j\}$, corresponding to optimally rotated Pauli operators (see also Figure 2).

Let us comment on some cases where our analysis is particularly effective. For GHZ states, cluster states, and half-excited Dicke states, which constitute primary resources for quantum computation and metrology [31, 32], we get the maximum $h_{\varpi} = 1$ for any even N . This means that our bounds remain robust to estimate global and partial entanglement in noisy versions of these states (i.e. when one considers mixtures of any of these states with probability q and the maximally mixed state with probability $1 - q$) for all $q > 1/3$. Notably, for values of q sufficiently close to 1, our bounds

N	State	$\{\tilde{c}_1, \tilde{c}_2, \tilde{c}_3\}$	$\sum_{j=1}^3 \tilde{c}_j $	$\{\theta, \psi, \phi\}$
≥ 3	$ \text{GHZ}^{(3)}\rangle$	$\left\{-\sqrt{\frac{8}{27}}, \sqrt{\frac{8}{27}}, -\sqrt{\frac{8}{27}}\right\}$	$2\sqrt{\frac{2}{3}}$	$\{\cos^{-1}(\frac{1}{\sqrt{3}}), \frac{5\pi}{30}, \frac{\pi}{4}\}$
$\leq N$	$ \text{W}^{(3)}\rangle$	$\left\{\frac{1}{\sqrt{3}}, -\frac{1}{\sqrt{3}}, \frac{1}{\sqrt{3}}\right\}$	$\sqrt{3}$	$\{\cos^{-1}(\frac{1}{\sqrt{3}}), 0, \frac{\pi}{4}\}$
	$ \text{GHZ}^{(4)}\rangle$	$\{1, 1, 1\}$	3	$\{0, 0, 0\}$
	$ \text{W}^{(4)}\rangle$	$\left\{\frac{5}{9}, \frac{5}{9}, \frac{5}{9}\right\}$	$\frac{5}{3}$	$\{\cos^{-1}(\frac{1}{\sqrt{3}}), 0, \frac{\pi}{4}\}$
≥ 4	$\varrho_{\text{Wei}}^{(4)}(x)$	$\{x, x, 2x-1\}$	$2x + 2x-1 $	$\{0, 0, 0\}$
$\leq N$	$ \text{C}_1^{(4)}\rangle$	$\{1, 1, 1\}$	3	*
	$ \text{C}_2^{(4)}\rangle$	$\{1, 1, 1\}$	3	$\{\frac{\pi}{4}, 0, 0\}$
	$ \text{D}_2^{(4)}\rangle$	$\{1, 1, 1\}$	3	$\{0, 0, 0\}$
	$ \Psi^{(4)}\rangle$	$\{1, 1, 1\}$	3	$\{0, 0, 0\}$
	$\varrho_S^{(4)}$	$\{1, 1, 1\}$	3	$\{0, 0, 0\}$
≥ 5	$ \text{GHZ}^{(5)}\rangle$	$\left\{\frac{1}{\sqrt{2}}, \frac{1}{\sqrt{2}}, 0\right\}$	$\sqrt{2}$	$\{0, \frac{\pi}{40}, \frac{\pi}{40}\}$
$\leq N$	$ \text{W}^{(5)}\rangle$	$\left\{\frac{7}{9\sqrt{3}}, -\frac{7}{9\sqrt{3}}, \frac{7}{9\sqrt{3}}\right\}$	$\frac{7}{3\sqrt{3}}$	$\{\cos^{-1}(\frac{1}{\sqrt{3}}), 0, \frac{\pi}{4}\}$
	$\varrho_{\text{Wei}}^{(5)}(x)$	$\left\{\frac{x}{\sqrt{2}}, \frac{x}{\sqrt{2}}, 0\right\}$	$\sqrt{2}x$	$\{0, \frac{\pi}{40}, \frac{\pi}{40}\}$
	$ \text{C}_1^{(5)}\rangle$	$\left\{\frac{1}{2}, \frac{1}{2}, \frac{1}{2}\right\}$	$\frac{3}{2}$	*
	$ \text{GHZ}^{(6)}\rangle$	$\{1, -1, 1\}$	3	$\{0, 0, 0\}$
≥ 6	$\varrho_{\text{Wei}}^{(6)}(x)$	$\{x, -x, 2x-1\}$	$2x + 2x-1 $	$\{0, 0, 0\}$
$\leq N$	$ \text{C}_1^{(6)}\rangle$	$\{1, -1, 1\}$	3	*
	$ \text{C}_2^{(6)}\rangle$	$\{1, -1, 1\}$	3	*
	$ \text{D}_3^{(6)}\rangle$	$\{1, 1, -1\}$	3	$\{0, 0, 0\}$
	$\varrho_S^{(6)}$	$\{-1, -1, -1\}$	3	$\{0, 0, 0\}$
≥ 7	$ \text{GHZ}^{(7)}\rangle$	$\left\{\frac{1}{\sqrt{2}}, -\frac{1}{\sqrt{2}}, 0\right\}$	$\sqrt{2}$	$\{0, \frac{\pi}{56}, \frac{\pi}{56}\}$
$\leq N$	$\varrho_{\text{Wei}}^{(7)}(x)$	$\left\{\frac{x}{\sqrt{2}}, -\frac{x}{\sqrt{2}}, 0\right\}$	$\sqrt{2}x$	$\{0, \frac{\pi}{56}, \frac{\pi}{56}\}$
	$ \text{C}_1^{(7)}\rangle$	$\left\{\frac{1}{2}, -\frac{1}{2}, \frac{1}{2}\right\}$	$\frac{3}{2}$	*
	$ \text{GHZ}^{(8)}\rangle$	$\{1, 1, 1\}$	3	$\{0, 0, 0\}$
≥ 8	$\varrho_{\text{Wei}}^{(8)}(x)$	$\{x, x, 2x-1\}$	$2x + 2x-1 $	$\{0, 0, 0\}$
$\leq N$	$ \text{C}_1^{(8)}\rangle$	$\{1, 1, 1\}$	3	*
	$ \text{D}_4^{(8)}\rangle$	$\{1, 1, 1\}$	3	$\{0, 0, 0\}$
	$\varrho_S^{(8)}$	$\{1, 1, 1\}$	3	$\{0, 0, 0\}$

to global entanglement can be tighter than the (more experimentally demanding) ones derived very recently in Ref. [23], as shown in Figure 3(a). Focusing on noisy GHZ states, we observe however that our scale-invariant threshold $q > 1/3$, obtained by measuring the three canonical Pauli operators for each qubit, is weaker than the well-established inseparability threshold $q > 1/(1 + 2^{N-1})$ [51]. Nevertheless, we note that our simple quantitative bound given by Eq. (4) becomes tight in the paradigmatic limit of pure GHZ states ($q = 1$) of any even number N of qubits, thus returning the *exact* value of their global multiparticle entanglement via Eq. (2), despite the fact that such states are not (and are very different from) \mathcal{M}_N^3 states. Eq. (4) also provides a useful nonvanishing lower bound to the global (and partial) N -particle entanglement of Wei states in the interval $x \in (\frac{1}{2}, 1]$, for any even N . A comparison between such a bound (with D denoting the relative entropy), which requires only three local measurements, and the true value of the relative entropy of global N -particle entanglement for these states [55], whose experimental evaluation would conventionally require a complete state tomography, is presented in Figure 3(b).

TABLE II. Applications of our method to construct accessible lower bounds on global and partial (M -inseparable) multiparticle entanglement (which are nonzero for any $M > \lceil N/2 \rceil$ when $\sum_j |\tilde{c}_j| > 1$), for the families of N -qubit states listed as follows. (i) N -qubit GHZ states [42] $|\text{GHZ}^{(N)}\rangle = \frac{1}{\sqrt{2}}(|00\cdots 00\rangle + |11\cdots 11\rangle)$ with $N \geq 3$. (ii) N -qubit W states [53] $|\text{W}^{(N)}\rangle = \frac{1}{\sqrt{N}}(|00\cdots 01\rangle + |00\cdots 10\rangle + \cdots + |10\cdots 00\rangle)$ with $N \geq 3$. (iii) N -qubit Wei states [54, 55] $\varrho_{\text{Wei}}^{(N)}(x) = x|\text{GHZ}^{(N)}\rangle\langle\text{GHZ}^{(N)}| + \frac{(1-x)}{2^N} \sum_{k=1}^N (P_k + \bar{P}_k)$, where $N \geq 4$, $x \in [0, 1]$ and P_k is the projector onto the binary N -qubit representation of 2^{k-1} whereas $\bar{P}_i = \sigma_1^{\otimes N} P_i \sigma_1^{\otimes N}$. (iv) N -qubit linear cluster states $|\text{C}_1^{(N)}\rangle$ corresponding to the N -vertex linear graph $\bullet - \bullet - \cdots - \bullet$ [21, 32]. (v) N -qubit rectangular cluster states $|\text{C}_2^{(N)}\rangle$ corresponding to the N -vertex ladder-type graph $\bullet - \bullet - \cdots - \bullet$ [32, 56]. (vi) N -qubit (symmetric) Dicke states $|\text{D}_k^{(N)}\rangle = \frac{1}{\sqrt{2}} \sum_i \Pi_i (|0\rangle^{\otimes N-k} \otimes |1\rangle^{\otimes k})$, which are superpositions of all states with k qubits in the excited state $|1\rangle$ and $N-k$ qubits in the ground state $|0\rangle$, with the symbol $\{\Pi_i(\cdot)\}_{i=1}^Z$ denoting all the $Z \equiv \binom{N}{k}$ distinct permutations of 0's and 1's; we focus on half-excited Dicke states, given by $k = N/2$ for any even N [46, 47, 57, 58]. (vii) 4-qubit singlet state [59] $|\Psi_4\rangle = \frac{1}{\sqrt{3}}(|0011\rangle + |1100\rangle - (|0101\rangle + |0110\rangle + |1001\rangle + |1010\rangle)/2$. (viii) N -qubit generalised Smolin states [38, 41, 60] $\varrho_S^{(N)}$ for even $N \geq 4$, which are instances of \mathcal{M}_N^3 states with correlation triple $\{(-1)^{N/2}, (-1)^{N/2}, (-1)^{N/2}\}$, hence their entanglement quantification is exact. The asterisk * indicates non-permutationally invariant states, for which the optimisation of the bounds requires different angles for each qubit (not reported here). Notice that in the table we listed mostly pure states. In general, if the triple $\{\tilde{c}_j\}$ is optimal for a pure N -qubit state $|\Phi^{(N)}\rangle$, then for the mixed state $\varrho^{(N)}(q) = q|\Phi^{(N)}\rangle\langle\Phi^{(N)}| + \frac{1-q}{2^N} \mathbb{I}^{\otimes N}$, obtained by mixing $|\Phi^{(N)}\rangle$ with white noise, one still gets nonzero lower bounds to global and partial entanglement for all $q > 1/\sum_{j=1}^3 |\tilde{c}_j|$, as shown in Figure 3 for some representative examples.

B. Genuine multiparticle entanglement

We now show how general analytical results for geometric measures of genuine multiparticle entanglement can be obtained as well within our approach. The results from the previous section, while quite versatile, cannot provide useful bounds for the complete hierarchy of multiparticle entanglement, because \mathcal{M}_N^3 states are M -separable for all $M \leq \lceil N/2 \rceil$, and thus in particular biseparable for any number N of qubits. Therefore, to investigate genuine entanglement we consider a different reference set of states, specifically formed by mixtures of GHZ states, hence incarnating archetypical representatives of full inseparability [11, 42]. Any such state ξ , which will be referred to as a GHZ-diagonal (in short, \mathcal{G}_N) state, can be written as $\xi = \sum_{i,\pm} p_i^\pm |\beta_i^\pm\rangle\langle\beta_i^\pm|$, in terms of its eigenvalues p_i^\pm , with the eigenvectors $|\beta_i^\pm\rangle = \frac{1}{\sqrt{2}}(|\mathbb{I}^{\otimes N} \pm \sigma_1^{\otimes N})|i\rangle$ forming a basis of N -qubit GHZ states (where $\{|i\rangle\}_{i=0}^{2^N-1}$ denotes the binary ordered N -qubit computational basis). The \mathcal{G}_N states have been studied in recent years as testbeds for multiparticle entanglement detection [11, 43], and specific algebraic measures of genuine multiparticle entanglement such

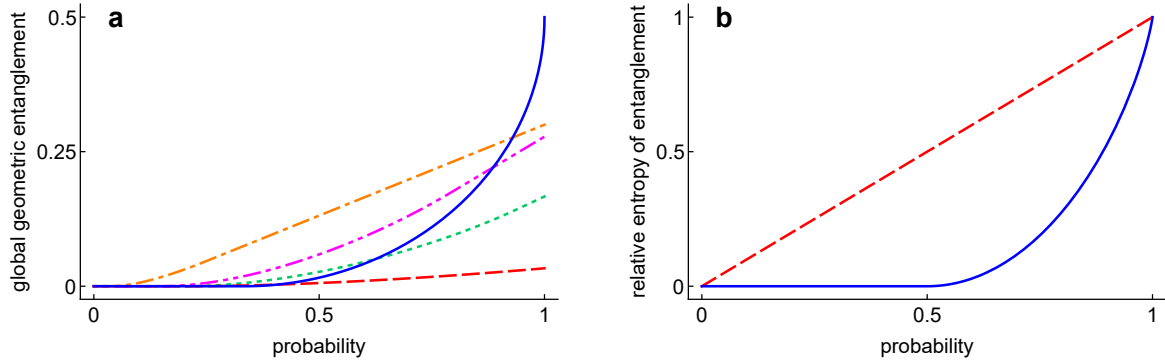


FIG. 3. (a) Lower bounds to the global geometric entanglement $E_N^{D_F}$ based on infidelity for noisy versions of some N -qubit states (defined in the caption of Table II), as functions of the probability q of obtaining the corresponding pure states. The non-solid lines refer to bounds obtained by the method of Ref. [23] for: 4-qubit linear cluster state (green dotted), 6-qubit rectangular cluster state (red dashed), 6-qubit half-excited Dicke state (orange dot-dashed), 4-qubit singlet state (magenta dot-dot-dashed). The solid blue line corresponds to our bound based on M_N^3 -fication for all the considered states, which is accessible by measuring only the three correlation functions $\tilde{c}_j = \langle \bigotimes_\alpha \tilde{\sigma}_j^{(\alpha)} \rangle$. (b) Relative entropy of multiparticle entanglement of N -qubit Wei states $\varrho_{\text{Wei}}^{(N)}$ defined in Table II, as a function of the probability x of obtaining a GHZ state. The dashed red line $E_N^{D_{\text{RE}}}(\varrho_{\text{Wei}}^{(N)}) = x$ denotes the exact value of the global relative entropy of entanglement as computed in [55]. The solid blue line denotes our accessible lower bound, obtained by combining Eqs. (2) and (5) with the expressions in Tables I and II, and given explicitly by $E_{N,\text{low}}^{D_{\text{RE}}}(\varrho_{\text{Wei}}^{(N)}) = \log_2(2 - 2x) + x(\log_2(x) - \log_2(1 - x))$ for $\frac{1}{2} < x \leq 1$, while it vanishes for $0 \leq x \leq \frac{1}{2}$. The bound becomes tight for $x = 1$, thus quantifying exactly the global multiparticle entanglement of pure GHZ states. We further show that our lower bound to global entanglement coincides with the exact genuine multiparticle entanglement of Wei states, $E_{N,\text{low}}^{D_{\text{RE}}}(\varrho_{\text{Wei}}^{(N)}) = E_2^{D_{\text{RE}}}(\varrho_{\text{Wei}}^{(N)})$, that is computed in the next section of this paper. The results are scale-invariant and hold for any even N .

as the N -particle concurrence [17, 19] and negativity [21] have been computed for these states. Here, we calculate exactly the whole class of geometric measures of genuine multiparticle entanglement E_2^D defined by Eq. (1), with respect to any contractive and jointly convex distance D , for \mathcal{G}_N states of an arbitrary number N of qubits.

By using analogous arguments to those in the previous section (see Supplementary Material), we can prove that, for every valid D , the closest biseparable state to any \mathcal{G}_N state can be found within the subset of biseparable \mathcal{G}_N states. The latter subset is well characterised [11], and is formed by all, and only, the \mathcal{G}_N states with eigenvalues such that $p_{\max} \equiv \max_{i,\pm} p_i^\pm \leq 1/2$. We can then show that the closest biseparable \mathcal{G}_N state to an arbitrary \mathcal{G}_N state has maximum eigenvalue equal to $1/2$, which allows us to solve the optimisation in the definition of E_2^D , with respect to every valid D . We have then a closed formula for the geometric multiparticle entanglement of any \mathcal{G}_N state ξ with maximum eigenvalue p_{\max} , given by

$$E_2^D(\xi^{(p_\pm^\pm)}) = \begin{cases} 0, & p_{\max} \leq 1/2; \\ g_D(p_{\max}), & \text{otherwise,} \end{cases} \quad (6)$$

where g_D denotes a monotonically increasing function whose explicit form is specific to each distance D , as reported in Table III for typical instances.

Let us comment on some particular results. The genuine multiparticle trace distance of entanglement $E_N^{D_{\text{Tr}}}$ is found to coincide with the genuine multiparticle negativity [21] and with half the genuine multiparticle concurrence [19] for all \mathcal{G}_N states, thus providing the latter entanglement measures with an insightful geometrical interpretation on this important set of states. Examples of \mathcal{G}_N states include several resources

Distance D	$g_D(p_{\max})$
Relative entropy D_{RE}	$1 + p_{\max} \log_2 p_{\max} + (1 - p_{\max}) \log_2(1 - p_{\max})$
Trace D_{Tr}	$p_{\max} - \frac{1}{2}$
Infidelity D_F	$\frac{1}{2} - \sqrt{p_{\max}(1 - p_{\max})}$
Squared Bures D_B	$2 - \sqrt{2} \left(\sqrt{1 - p_{\max}} + \sqrt{p_{\max}} \right)$
Squared Hellinger D_H	$2 - \sqrt{2} \left(\sqrt{1 - p_{\max}} + \sqrt{p_{\max}} \right)$

TABLE III. Analytical expression of genuine multiparticle entanglement E_2^D for GHZ-diagonal states of any number N of qubits as defined by Eq. (6), for representative choices of the distance function D (introduced in Table I).

for quantum information processing, such as the noisy GHZ states and Wei states introduced in the previous section. In particular, for noisy GHZ states (described by a pure-state probability q as detailed in Table II), we recover that every geometric measure of genuine multiparticle entanglement is nonzero if and only if $q > (1 + (1 - 2^N)^{-1})/2 \xrightarrow{N \gg 1} 1/2$ [19, 43] and monotonically increasing with q , as expected; for $q = 1$ (pure GHZ states), genuine and global entanglement coincide, i.e. the hierarchy of Figure 1 collapses, meaning that all the entanglement of N -qubit GHZ states is genuinely shared among all the N particles [26]. On the other hand, the relative entropy of genuine multiparticle entanglement of Wei states [54, 55] can be calculated exactly via Eq. (6); interestingly, for even N it is found to coincide with the lower bound

to their global entanglement that we had obtained by \mathcal{M}_N^3 -fication, plotted as a solid line in Figure 3(b). This means that for these states also the genuine multiparticle entanglement can be quantified entirely by measuring the three canonical correlation functions $\{c_j\}$, for any N . More generally, for arbitrary \mathcal{G}_N states, all the genuine entanglement measures given by Eq. (6) can be obtained by measuring the maximum GHZ overlap p_{\max} , which requires $N + 1$ local measurement settings given explicitly in Ref. [43]. This is remarkable, since with the same experimental effort needed to detect full inseparability [11] we have now a complete quantitative picture of genuine entanglement in these states; furthermore, as evident from Eq. (6), all the geometric measures are monotonic functions of each other: our analysis thus reveals that there is a unique ordering of genuinely entangled \mathcal{G}_N states within the distance-based approach of Fig. 1.

In the same spirit as the previous section, we note that the exact results obtained for the particular reference family of \mathcal{G}_N states provide quantitative lower bounds to the genuine entanglement of general N -qubit states. This follows from the observation that any N -qubit state ϱ can be transformed into a \mathcal{G}_N state with eigenvalues $p_i^\pm = \langle \beta_i^\pm | \varrho | \beta_i^\pm \rangle$ by a procedure that we may call GHZ-diagonalisation, amounting to local operations and classical communication [21]. Therefore, given a completely general state ϱ , one only needs to measure its overlap with a suitable reference GHZ state; if this overlap is found larger than $1/2$, then by using Eq. (6) with p_{\max} equal to the measured overlap one obtains analytical lower bounds to the genuine multiparticle entanglement E_2^D of ϱ with respect to any desired distance D . As before, the bounds can be optimised in situations of partial prior knowledge, e.g. by applying local unitaries on each qubit before the GHZ-diagonalisation, which has the effect of maximising the overlap with a chosen particular GHZ vector in the basis $\{|\beta_i^\pm\rangle\}$. The bounds then remain accessible for any state ϱ by $N + 1$ local measurements [43], with exactly the same demand as for just witnessing entanglement [11].

For instance, for the singlet state $|\Psi^{(4)}\rangle$ [59], which is a relevant resource in a number of quantum protocols including multiuser secret sharing [64–66], one has $p_{\max} = \langle \beta_3^+ | \Psi^{(4)} \rangle \langle \Psi^{(4)} | \beta_3^+ \rangle = 2/3 > 1/2$, obtainable by measuring the overlap with the GHZ basis state $|\beta_3^+\rangle = (|0011\rangle + |1100\rangle)/\sqrt{2}$. Optimised bounds to the genuine multiparticle entanglement of half-excited Dicke states $|\mathcal{D}_{N/2}^{(N)}\rangle$ (for even $N \geq 4$), defined in Table II [57, 58], can be found as well based on GHZ-diagonalisation, and are expressed by $p_{\max}^{(N)} = \binom{N}{N/2} 2^{1-N}$, meaning that they become looser with increasing N and stay nonzero only up to $N = 8$. In this respect, we note that alternative methods to detect full inseparability of Dicke states for any N are available [3, 46, 47], but quantitative results are lacking in general.

Finally, notice that a lower bound to a distance-based measure of genuine multiparticle entanglement, as derived in this section, is automatically also a lower bound to corresponding measures of global and any form of partial entanglement, as evident by looking at the geometric picture in Figure 1. However, for states which are entangled yet not genuinely entangled, the simple bound from the previous section remains in-

strumental to assess their inseparability with minimum effort. \mathcal{M}_N^3 states are themselves instances of such states (in fact, for even N , \mathcal{M}_N^3 states are also \mathcal{G}_N states, but with $p_{\max} \leq 1/2$).

C. Applications to experimental states

In this section, we benchmark the applicability of our methods to *real data* from recent experiments [39, 44–47, 67].

In Refs. [39, 40], the authors used quantum optical setups to prepare an instance of a bound entangled four-qubit state, known as Smolin state [60]. Such a state cannot be written as a convex mixture of product states of the four qubits, yet no entanglement can be distilled out of it, thus incarnating the irreversibility in entanglement manipulation while still representing a useful resource for information locking and quantum secret sharing [5, 41]. It turns out that noisy Smolin states are particular types of \mathcal{M}_N^3 states (for any even N) [38, 41], that in the representation of Figure 2(b) are located along the segment connecting the tetrahedron vertex $\{(-1)^{N/2}, (-1)^{N/2}, (-1)^{N/2}\}$ with the origin. Therefore, this work provides exact analytical formulae for all the nontrivial hierarchy of their global and partial entanglement, as mentioned in Table II. In the specific experimental implementation of Ref. [39] for $N = 4$, the global entanglement was detected (but not quantified) via a witness constructed by measuring precisely the three correlation functions $\{c_j\}$. Based on the existing data alone (and without assuming that the produced state is within the \mathcal{M}_N^3 family), we can then provide a quantitative estimate to the multiparticle entanglement of this experimental bound entangled state in terms of any geometric measure E_M^D , by using Table I. The results are reported in Table IV(a) for the illustrative case of the trace distance.

Remaining within the domain of quantum optics, recently two laboratories reported the creation of six-photon Dicke states $|\mathcal{D}_3^{(6)}\rangle$ [46, 47]. Dicke states [57] are valuable resources for quantum metrology, computation, and networked communication, and emerge naturally in many-body systems as ground states of the isotropic Lipkin-Meshkov-Glick model [58]. Based on the values of the three correlation functions $\{c_j\}$, which were measured in Refs. [46, 47] to construct some entanglement witnesses, we can provide quantitative bounds to their global and partial geometric entanglement E_M^D (for $4 \leq M \leq 6$) from Eq. (4); see Table IV(a).

A series of experiments at Innsbruck [35, 44, 45, 67] has resulted in the generation of a variety of relevant multi-qubit states with trapped ion setups, for explorations of fundamental science and for the implementation of quantum protocols. In those realisations, data acquisition and processing for the purpose of entanglement verification was often a more demanding task than running the experiment itself [44]. Focusing first on global and partial entanglement, we obtained full datasets for experimental density matrices corresponding to particularly noisy GHZ and W states of up to four qubits, produced during laboratory test runs [67]. Despite the relatively low fidelity with their ideal target states, we still obtain meaningful quantitative bounds from Eq. (5). The results are compactly presented in Table IV(a).

Global and partial multiparticle entanglement					
State	Ref.	Fidelity (%)	$\{\tilde{c}_1, \tilde{c}_2, \tilde{c}_3\}$	$\sum_{j=1}^3 \tilde{c}_j $	$E_M^{D_{\text{Tr}}}$
$\varrho_{S}^{(4)}$	[39]	96.83 ± 0.05	$\{0.401 \pm 0.004, 0.362 \pm 0.004, 0.397 \pm 0.008\}$	1.16 ± 0.01	0.040 ± 0.002
$\varrho_{D_3}^{(6)}$	[46]	56 ± 2	$\{0.8 \pm 0.2, 0.5 \pm 0.2, -0.3 \pm 0.1\}$	1.6 ± 0.3	0.15 ± 0.08
$\varrho_{D_3}^{(6)}$	[47]	65 ± 2	$\{0.63 \pm 0.02, 0.63 \pm 0.02, -0.42 \pm 0.02\}$	1.69 ± 0.04	0.17 ± 0.01
$\varrho_{\text{GHZ}}^{(3)}$	[67]	87.9	$\{-0.497, 0.515, -0.341\}$	1.35	0.102
$\varrho_{\text{GHZ}}^{(4)}$	[67]	80.3	$\{0.663, 0.683, 0.901\}$	2.25	0.312
$\varrho_{W_A}^{(4)}$	[67]	19.4	$\{-0.404, 0.454, -0.378\}$	1.24	0.0589
$\varrho_{W_B}^{(4)}$	[67]	31.4	$\{0.472, -0.468, -0.446\}$	1.39	0.0963

Genuine multiparticle entanglement					
State	Ref.	Fidelity (%)	$E_2^{D_{\text{RE}}}$	$E_2^{D_{\text{Tr}}}$	$E_2^{D_{\text{F}}}$
$\varrho_{\text{GHZ}}^{(3)}$	[45]	97.0 ± 0.3	0.81 ± 0.02	0.470 ± 0.003	0.329 ± 0.008
$\varrho_{\text{GHZ}}^{(4)}$	[45]	95.7 ± 0.3	0.74 ± 0.01	0.457 ± 0.003	0.297 ± 0.007
$\varrho_{\text{GHZ}}^{(5)}$	[45]	94.4 ± 0.5	0.69 ± 0.02	0.444 ± 0.005	0.27 ± 0.01
$\varrho_{\text{GHZ}}^{(6)}$	[45]	89.2 ± 0.4	0.51 ± 0.01	0.392 ± 0.004	0.190 ± 0.005
$\varrho_{\text{GHZ}}^{(8)}$	[45]	81.7 ± 0.4	0.313 ± 0.009	0.317 ± 0.004	0.113 ± 0.003
$\varrho_{\text{GHZ}}^{(10)}$	[45]	62.6 ± 0.6	0.046 ± 0.004	0.126 ± 0.006	0.016 ± 0.002
$\varrho_{\text{GHZ}}^{(14)}$	[45]	50.8 ± 0.9	0.0002 ± 0.0004	0.008 ± 0.009	0.0001 ± 0.0001

TABLE IV. (a) Accessible lower bounds to global and partial multiparticle entanglement of some experimentally prepared states, given by Eq. (5) and evaluated in particular for the trace distance of entanglement $E_M^{D_{\text{Tr}}}$ by using Eq. (2) for even N and Eq. (3) for odd N . Following the theoretical analysis of Table II, data obtained by direct measurements of the canonical correlation functions were used to construct bounds for a noisy Smolin state of 4 photons [39], noisy Dicke states of 6 photons [46, 47], and noisy GHZ states of 4 ions [67]. For noisy GHZ states of 3 ions and noisy W states of 4 ions (two implementations labelled as A and B) [67], full datasets were used to extract the optimised correlation functions $\{\tilde{c}_j\}$ required for the bounds. For all the presented experimental states (whose fidelities with the ideal target states are reported for reference), we are able to provide a reliable estimate of the multiparticle entanglement E_M^D for any $M > \lceil N/2 \rceil$. (b) Lower bounds to genuine multiparticle entanglement of experimental noisy GHZ states of up to 14 ions [45], as quantified in terms of all the distance-based entanglement measures E_2^D reported in Table III, obtained by Eq. (6) with p_{\max} given in each case by the measured fidelity with the pure reference GHZ state. All the reported entanglement estimates are obtained from the same data needed to witness full inseparability, which for general N -qubit states can be accessed by $N + 1$ local measurements without the need for a full tomography.

Regarding now genuine multiparticle entanglement, the authors of Ref. [45] reported the creation of (noisy) GHZ states of up to $N = 14$ trapped ions. In each of these states, full inseparability was witnessed by measuring precisely the maximum overlap p_{\max} with a reference pure GHZ state, without the need for complete state tomography. Thanks to Eq. (6), we can now use the same data to obtain a full quantification of the genuine N -particle entanglement of these realistic states, according to any measure E_2^D , at no extra cost in terms of experimental or computational resources. The results are in Table IV(b), for all the representative choices of distances enumerated in Table III. Notice that we do not need to assume that the experimentally produced states are in the \mathcal{G}_N set: the obtained results can be still safely regarded as lower bounds.

III. DISCUSSION

We have achieved a compendium of exact results on the quantification of general distance-based measures of (global, partial, and genuine) multiparticle entanglement in some pivotal reference families of N -qubit mixed states. This allowed us to establish faithful lower bounds to various forms of multiparticle entanglement for general states, accessible by few local measurements and effective on prominent resource states for quantum information processing.

Our approach can be regarded as realising simple yet particularly convenient instances of quantitative entanglement witnesses [49, 50], with the crucial advance that our lower bounds are analytical (in contrast to conventional numerical approaches requiring semidefinite programming) and hold for *all* valid geometric measures of entanglement, which are endowed with meaningful operational interpretations yet have been traditionally hard to evaluate [22, 23].

A key aspect of our analysis lies in fact in the generality of the adopted techniques, which rely on natural information-theoretic requirements of contractivity and joint convexity of any distance D entering Eq. (1). We can expect our methods to be applicable to other reference sets of states (for example, states diagonal in a basis of cluster states [21, 22], or more general states with X-shaped density matrices [19]), thereby leading to alternative entanglement bounds for general states, which might be more tailored to different classes, or to specific measurement settings in laboratory.

Another key feature of our framework is its accessibility. Having tested our entanglement bounds on a selection of very different families of theoretical and experimentally produced states with high levels of noise, we can certify their usefulness in realistic scenarios. We recall that, for instance, three canonical local measurements suffice to quantify exactly the global entanglement of GHZ states of any even number N of qubits, while $N + 1$ local measurements provide their exact

genuine entanglement, according to every geometric measure for any N , when such states are realistically mixed with white noise. This can lead to a considerable simplification of future experiments based on these archetypical resources, involving e.g. two quantum bytes (16 qubits) and beyond [45, 67].

In subsequent works, we plan to extend our analysis in order to obtain accessible analytical results for the geometric quantification of other useful forms of multiparticle quantum correlations, such as Einstein-Podolsky-Rosen steering [68, 69], and Bell nonlocality in many-body systems [58]. This can eventually lead to a unifying characterisation, resting on the framework of information geometry, of the whole spectrum of genuine signatures of quantumness in cooperative phenomena.

IV. METHODS

Distance-based measures of multiparticle entanglement.

A general distance-based measure of multiparticle entanglement E_M^D is defined in Eq. (1). In this work, the distance D is required to satisfy the following two physical constraints:

- (D.i) Contractivity under quantum channels, i.e. $D(\Omega(\varrho), \Omega(\varrho')) \leq D(\varrho, \varrho')$, for any states ϱ, ϱ' , and any completely positive trace preserving map Ω ;
- (D.ii) Joint convexity, i.e. $D(q\varrho + (1-q)\varrho', q\chi + (1-q)\chi') \leq qD(\varrho, \chi) + (1-q)D(\varrho', \chi')$, for any states $\varrho, \varrho', \chi, \chi'$, and any $q \in [0, 1]$.

Constraint (D.i) implies that E_M^D is invariant under local unitaries and monotonically nonincreasing under local operations and classical communication (i.e., it is an entanglement monotone [4]). Constraint (D.ii) implies that E_M^D is also convex. A selection of distance functionals respecting these properties is given in Table I.

\mathcal{M}_N^3 -fication. *Theorem.* Any N -qubit state ϱ can be transformed into a corresponding \mathcal{M}_N^3 state ϖ through a fixed transformation, Θ , consisting of single-qubit local operations and classical communication, such that $\Theta(\varrho) = \varpi = \frac{1}{2^N} (\mathbb{I}^{\otimes N} + \sum_{i=1}^3 c_i \sigma_i^{\otimes N})$, where $c_i = \text{Tr}(\varrho \sigma_i^{\otimes N})$.

Proof. Here we sketch the form of the \mathcal{M}_N^3 -fication channel Θ . We begin by setting $2(N-1)$ single-qubit local unitaries $\{U_j\}_{j=1}^{2(N-1)} = \{(\sigma_1 \otimes \sigma_1 \otimes \mathbb{I}^{\otimes N-2}), (\mathbb{I} \otimes \sigma_1 \otimes \sigma_1 \otimes \mathbb{I}^{\otimes N-3}), \dots, (\mathbb{I}^{\otimes N-3} \otimes \sigma_1 \otimes \sigma_1 \otimes \mathbb{I}), (\mathbb{I}^{\otimes N-2} \otimes \sigma_1 \otimes \sigma_1), (\sigma_2 \otimes \sigma_2 \otimes \mathbb{I}^{\otimes N-2}), (\mathbb{I} \otimes \sigma_2 \otimes \sigma_2 \otimes \mathbb{I}^{\otimes N-3}), \dots, (\mathbb{I}^{\otimes N-3} \otimes \sigma_2 \otimes \sigma_2 \otimes \mathbb{I}), (\mathbb{I}^{\otimes N-2} \otimes \sigma_2 \otimes \sigma_2)\}$. Then, we fix a sequence of states $\{\varrho_0, \varrho_1, \dots, \varrho_{2(N-1)}\}$ defined by $\varrho_j = \frac{1}{2} (\varrho_{j-1} + U_j \varrho_{j-1} U_j^\dagger)$, for $j \in \{1, 2, \dots, 2(N-1)\}$. By setting $\varrho_0 = \varrho$ and $\varrho_{2(N-1)} = \Theta(\varrho)$, we define the required channel: $\Theta(\varrho) = \frac{1}{2^{2(N-1)}} \sum_{i=1}^{2^{2(N-1)}} U'_i \varrho U'_i$, where: $\{U'_i\}_{i=1}^{2^{2(N-1)}} = \{\mathbb{I}^{\otimes N}, \{U_{i_1}\}_{i_1=1}^{2(N-1)}, \{U_{i_2} U_{i_1}\}_{i_2>i_1=1}^{2(N-1)}, \dots, \{U_{i_{2(N-1)}} \dots U_{i_2} U_{i_1}\}_{i_{2(N-1)}>\dots>i_2>i_1=1}^{2(N-1)}\}$. Notice that $\{U'_i\}_{i=1}^{2^{2(N-1)}}$ is still a sequence of single-qubit local unitaries. Since Θ is a convex mixture of such local unitaries, it belongs to the class

of single-qubit local operations and classical communication, mapping any M -separable set into itself. In the Supplementary Material, we show that $\Theta(\varrho) = \varpi$, concluding the proof.

Lower bound optimisation. For any valid distance-based measure of global and partial multiparticle entanglement E_M^D , the maximisation in Eq. (5) is equivalent (for even N) to maximising $|\tilde{c}_1| + |\tilde{c}_2| + |\tilde{c}_3|$, where $\tilde{c}_j = \text{Tr}[U_{\otimes} \varrho U_{\otimes}^\dagger \sigma_j^{\otimes N}]$, over local single-qubit unitaries $U_{\otimes} = \bigotimes_{\alpha=1}^N U^{(\alpha)}$ ($\alpha = 1, \dots, N$). By using the well known correspondence between the special unitary group $\text{SU}(2)$ and special orthogonal group $\text{SO}(3)$, we have that to any one-qubit unitary $U^{(\alpha)}$ corresponds the orthogonal 3×3 matrix $O^{(\alpha)}$ such that $U^{(\alpha)} \vec{n} \cdot \vec{\sigma} U^{(\alpha)\dagger} = (O^{(\alpha)} \vec{n}) \cdot \vec{\sigma}$, where $\vec{n} = \{n_1, n_3, n_3\} \in \mathbb{R}^3$ and $\vec{\sigma} = \{\sigma_1, \sigma_2, \sigma_3\}$ is the vector of Pauli matrices. We have then that $\sup_{\{U^{(\alpha)}\}} (|\tilde{c}_1| + |\tilde{c}_2| + |\tilde{c}_3|) = \sup_{\{O^{(\alpha)}\}} (|\tilde{T}_{11\dots1}| + |\tilde{T}_{22\dots2}| + |\tilde{T}_{33\dots3}|)$, where $\tilde{T}_{i_1 i_2 \dots i_N} = \sum_{j_1 j_2 \dots j_N} T_{j_1 j_2 \dots j_N} O_{i_1 j_1}^{(1)} O_{i_2 j_2}^{(2)} \dots O_{i_N j_N}^{(N)}$, and $T_{i_1 i_2 \dots i_N} = \text{Tr}[\varrho (\sigma_{i_1} \otimes \sigma_{i_2} \otimes \dots \otimes \sigma_{i_N})]$. In the case of permutationally invariant states ϱ , the $3 \times 3 \times \dots \times 3$ tensor $T_{i_1 i_2 \dots i_N}$ is fully symmetric, i.e. $T_{i_1 i_2 \dots i_N} = T_{\vartheta(i_1 i_2 \dots i_N)}$ for any permutation ϑ of the indices, so that the optimisation can be achieved when $O^{(1)} = O^{(2)} = \dots = O^{(N)}$ [70]. As indicated in the main text, we then need to perform the maximisation over just the three angles $\{\theta, \psi, \phi\}$ which determine the orthogonal matrix $O^{(\alpha)}$ corresponding to an arbitrary single-qubit unitary

$$U^{(\alpha)} = \begin{pmatrix} \cos \frac{\theta}{2} e^{-i \frac{\psi+\phi}{2}} & -i \sin \frac{\theta}{2} e^{-i \frac{\phi-\psi}{2}} \\ -i \sin \frac{\theta}{2} e^{i \frac{\phi-\psi}{2}} & \cos \frac{\theta}{2} e^{i \frac{\psi+\phi}{2}} \end{pmatrix}.$$

As a special case, for a two-qubit state ($N = 2$) the optimal local operation is the one which diagonalises the correlation matrix $(T_{i_1 i_2})$.

ACKNOWLEDGMENTS

We warmly thank Thomas Monz, Mauro Paternostro, Christian Schwemmer, and Witlef Wieczorek for providing experimental data, and we acknowledge fruitful discussions with (in alphabetical order) I. Almeida Silva, M. Blasone, D. Cavalcanti, E. Carnio, T. Chanda, M. Christandl, P. Comon, M. Cramer, M. Gessner, T. Ginestra, D. Gross, O. Gühne, M. Guta, M. Huber, F. Illuminati, I. Kogias, T. Kypraios, P. Liuzzo-Scorpo, C. Macchiavello, A. Milne, T. Monz, P. Ott, A. K. Pal, M. Piani, M. Prater, S. Rat, A. Sanpera, P. Skrzypczyk, A. Streltsov, G. Toth, A. Winter. This work was supported by the European Research Council (ERC) Starting Grant GQCOP, Grant Agreement No. 637352.

M. C. and T. R. B. contributed equally to this work.

CORRESPONDING AUTHOR

Correspondence to:
Gerardo Adesso (gerardo.adesso@nottingham.ac.uk)

[1] Einstein, A., Podolsky, B. & Rosen, N. Can quantum-mechanical description of physical reality be considered complete? *Phys. Rev.* **47**, 777–780 (1935).

[2] Vedral, V. Quantum entanglement. *Nat. Phys.* **10**, 256–258 (2014).

[3] Gühne, O. & Tóth, G. Entanglement detection. *Phys. Rep.* **474**, 1–75 (2009).

[4] Plenio, M. B. & Virmani, S. An introduction to entanglement measures. *Quant. Inf. Comput.* **7**, 1 (2007).

[5] Horodecki, R., Horodecki, P., Horodecki, M. & Horodecki, K. Quantum entanglement. *Rev. Mod. Phys.* **81**, 865–942 (2009).

[6] Sarovar, M., Ishizaki, A., Fleming, G. R. & Whaley, K. B. Quantum entanglement in photosynthetic light-harvesting complexes. *Nat. Phys.* **6**, 462–467 (2010).

[7] Cramer, M., Plenio, M. B. & Wunderlich, H. Measuring entanglement in condensed matter systems. *Phys. Rev. Lett.* **106**, 020401 (2011).

[8] Cramer, M. *et al.* Spatial entanglement of bosons in optical lattices. *Nat. Commun.* **4**, 2161 (2013).

[9] Marty, O. *et al.* Quantifying entanglement with scattering experiments. *Phys. Rev. B* **89**, 125117 (2014).

[10] Marty, O., Cramer, M. & Plenio, M. B. Practical entanglement estimation for spin-system quantum simulators (2015). arXiv:1504.03572.

[11] Gühne, O. & Seevinck, M. Separability criteria for genuine multipartite entanglement. *New J. Phys.* **12**, 053002 (2010).

[12] Huber, M., Mintert, F., Gabriel, A. & Hiesmayr, B. C. Detection of high-dimensional genuine multipartite entanglement of mixed states. *Phys. Rev. Lett.* **104**, 210501 (2010).

[13] Kraus, B. Local unitary equivalence of multipartite pure states. *Phys. Rev. Lett.* **104**, 020504 (2010).

[14] Levi, F. & Mintert, F. Hierarchies of multipartite entanglement. *Phys. Rev. Lett.* **110**, 150402 (2013).

[15] Gao, T., Yan, F. & van Enk, S. J. Permutationally invariant part of a density matrix and nonseparability of n -qubit states. *Phys. Rev. Lett.* **112**, 180501 (2014).

[16] Klöckl, C. & Huber, M. Characterizing multipartite entanglement without shared reference frames. *Phys. Rev. A* **91**, 042339 (2015).

[17] Ma, Z.-H. *et al.* Measure of genuine multipartite entanglement with computable lower bounds. *Phys. Rev. A* **83**, 062325 (2011).

[18] Wu, J.-Y., Kampermann, H., Bruß, D., Klöckl, C. & Huber, M. Determining lower bounds on a measure of multipartite entanglement from few local observables. *Phys. Rev. A* **86**, 022319 (2012).

[19] Hashemi Rafsanjani, S. M., Huber, M., Broadbent, C. J. & Eberly, J. H. Genuinely multipartite concurrence of n -qubit x matrices. *Phys. Rev. A* **86**, 062303 (2012).

[20] Eltschka, C. & Siewert, J. A quantitative witness for greenberger-horne-zeilinger entanglement. *Sci. Rep.* **2** (2012).

[21] Hofmann, M., Moroder, T. & Gühne, O. Analytical characterization of the genuine multipartite negativity. *J. Phys. A: Math. Theor.* **47**, 155301 (2014).

[22] Chen, X.-y., Yu, P., Jiang, L.-z. & Tian, M. Genuine entanglement of four-qubit cluster diagonal states. *Phys. Rev. A* **87**, 012322 (2013).

[23] Buchholz, L. E., Moroder, T. & Gühne, O. Evaluating the geometric measure of multiparticle entanglement (2014). arXiv:1412.7471.

[24] Vedral, V., Plenio, M. B., Rippin, M. A. & Knight, P. L. Quantifying entanglement. *Phys. Rev. Lett.* **78**, 2275–2279 (1997).

[25] Wei, T.-C. & Goldbart, P. M. Geometric measure of entanglement and applications to bipartite and multipartite quantum states. *Phys. Rev. A* **68**, 042307 (2003).

[26] Blasone, M., Dell’Anno, F., De Siena, S. & Illuminati, F. Hierarchies of geometric entanglement. *Phys. Rev. A* **77**, 062304 (2008).

[27] Bengtsson, I. & Zyczkowski, K. *Geometry of Quantum States: An Introduction to Quantum Entanglement* (Cambridge University Press, 2006).

[28] Wei, T.-C., Das, D., Mukhopadhyay, S., Vishveshwara, S. & Goldbart, P. M. Global entanglement and quantum criticality in spin chains. *Phys. Rev. A* **71**, 060305 (2005).

[29] Biham, O., Nielsen, M. A. & Osborne, T. J. Entanglement monotone derived from grover’s algorithm. *Phys. Rev. A* **65**, 062312 (2002).

[30] Bell, B. A. *et al.* Spatial entanglement of bosons in optical lattices. *Nat. Commun.* **5**, 5480 (2014).

[31] Giovannetti, V., Lloyd, S. & Maccone, L. Advances in quantum metrology. *Nat. Photon.* **5**, 222 (2011).

[32] Briegel, H. J., Browne, D. E., Dür, W., Raussendorf, R. & den Nest, M. V. *Nat. Phys.* **5**, 19–26 (2009).

[33] Gabriel, A., Hiesmayr, B. C. & Huber, M. Criterion for k -separability in mixed multipartite systems. *Quantum Information and Computation* **10**, 829–836 (2010).

[34] Tiersch, M., Popescu, S. & Briegel, H. J. A critical view on transport and entanglement in models of photosynthesis. *Phil. Trans. Roy. Soc. A* **370**, 3771–3786 (2012).

[35] Barreiro, J. T. *et al.* Experimental multiparticle entanglement dynamics induced by decoherence. *Nat. Phys.* **6**, 943 (2010).

[36] Hayashi, M., Markham, D., Murao, M., Owari, M. & Virmani, S. Bounds on multipartite entangled orthogonal state discrimination using local operations and classical communication. *Phys. Rev. Lett.* **96**, 040501 (2006).

[37] Streltsov, A., Kampermann, H. & Bruß, D. Linking a distance measure of entanglement to its convex roof. *New J. Phys.* **12**, 123004 (2010).

[38] Hiesmayr, B. C., Hipp, F., Huber, M., Krammer, P. & Spengler, C. Simplex of bound entangled multipartite qubit states. *Phys. Rev. A* **78**, 042327 (2008).

[39] Lavoie, J., Kaltenbaek, R., Piani, M. & Resch, K. J. Experimental bound entanglement in a four-photon state. *Phys. Rev. Lett.* **105**, 130501 (2010).

[40] Amselem, E. & Bourennane, M. Experimental four-qubit bound entanglement. *Nat. Phys.* **5**, 748 (2009).

[41] Augusiak, R. & Horodecki, P. Generalized smolin states and their properties. *Physical Review A* **73**, 012318 (2006).

[42] Greenberger, D. M., Horne, M. & Zeilinger, A. *Am. J. Phys.* **58**, 1131 (1990).

[43] Gühne, O., Lu, C.-Y., Gao, W.-B. & Pan, J.-W. Toolbox for entanglement detection and fidelity estimation. *Phys. Rev. A* **76**, 030305 (2007).

[44] Häffner, H. *et al.* Scalable multiparticle entanglement of trapped ions. *Nature* **438**, 643–646 (2005).

[45] Monz, T. *et al.* 14-qubit entanglement: Creation and coherence. *Phys. Rev. Lett.* **106**, 130506 (2011).

[46] Prevedel, R. *et al.* Experimental realization of dicke states of up to six qubits for multiparty quantum networking. *Phys. Rev. Lett.* **103**, 020503 (2009).

[47] Wieczorek, W. *et al.* Experimental entanglement of a six-photon symmetric dicke state. *Phys. Rev. Lett.* **103**, 020504 (2009).

[48] Badziąg, P., Brukner, Ć., Laskowski, W., Paterek, T. & Żukowski, M. Experimentally friendly geometrical criteria for entanglement. *Phys. Rev. Lett.* **100**, 140403 (2008).

[49] Eisert, J., Brandão, F. G. & Audenaert, K. M. Quantitative entanglement witnesses. *New J. Phys.* **9**, 46 (2007).

[50] Gühne, O., Reimpell, M. & Werner, R. F. Estimating entanglement measures in experiments. *Phys. Rev. Lett.* **98**, 110502 (2007).

[51] Dür, W. & Cirac, J. I. Classification of multiqubit mixed states: Separability and distillability properties. *Phys. Rev. A* **61**, 042314 (2000).

[52] Carnio, E. G., Buchleitner, A. & Gessner, M. Robust asymptotic entanglement under multipartite collective dephasing. *Phys. Rev. Lett.* **115**, 010404 (2015).

[53] Dür, W., Vidal, G. & Cirac, J. I. Three qubits can be entangled in two inequivalent ways. *Phys. Rev. A* **62**, 062314 (2000).

[54] Wei, T. C., Altepeter, J. B., Goldbart, P. M. & Munro, W. J. Measures of entanglement in multipartite bound entangled states. *Phys. Rev. A* **70**, 022322 (2004).

[55] Wei, T.-C. Relative entropy of entanglement for multipartite mixed states: Permutation-invariant states and dür states. *Phys. Rev. A* **78**, 012327 (2008).

[56] Raussendorf, R. & Briegel, H. J. A one-way quantum computer. *Phys. Rev. Lett.* **86**, 5188–5191 (2001).

[57] Dicke, R. H. Coherence in spontaneous radiation processes. *Phys. Rev.* **93**, 99–110 (1954).

[58] Tura, J. *et al.* Detecting nonlocality in many-body quantum states. *Science* **344**, 1256–1258 (2014).

[59] Weinfurter, H. & Żukowski, M. Four-photon entanglement from down-conversion. *Physical Review A* **64**, 010102 (2001).

[60] Smolin, J. A. Four-party unlockable bound entangled state. *Phys. Rev. A* **63**, 032306 (2001).

[61] Cabello, A. Solving the liar detection problem using the four-qubit singlet state. *Phys. Rev. A* **68**, 012304 (2003).

[62] Kiesel, N. *et al.* Experimental analysis of a four-qubit photon cluster state. *Phys. Rev. Lett.* **95**, 210502 (2005).

[63] Kiesel, N., Schmid, C., Tóth, G., Solano, E. & Weinfurter, H. Experimental observation of four-photon entangled dicke state with high fidelity. *Phys. Rev. Lett.* **98**, 063604 (2007).

[64] Bourennane, M. *et al.* Decoherence-free quantum information processing with four-photon entangled states. *Physical review letters* **92**, 107901 (2004).

[65] Murao, M., Jonathan, D., Plenio, M. & Vedral, V. Quantum telecloning and multiparticle entanglement. *Physical Review A* **59**, 156 (1999).

[66] Gaertner, S., Kurtsiefer, C., Bourennane, M. & Weinfurter, H. Experimental demonstration of four-party quantum secret sharing. *Physical Review Letters* **98**, 020503 (2007).

[67] Monz, T. *Quantum information processing beyond ten ion qubits*. Ph.D. thesis, Institute for Experimental Physics, University of Innsbruck (2011).

[68] Wiseman, H. M., Jones, S. J. & Doherty, A. C. Steering, entanglement, nonlocality, and the einstein-podolsky-rosen paradox. *Phys. Rev. Lett.* **98**, 140402 (2007).

[69] Armstrong, S. *et al.* Multipartite einstein-podolsky-rosen steering and genuine tripartite entanglement with optical networks. *Nat. Phys.* **11**, 167 (2015).

[70] Comon, P. & Sørensen, M. Tensor diagonalization by orthogonal transforms. *Report ISRN IIS-RR-2007-06-FR* (2007).

Accessible quantification of multiparticle entanglement

SUPPLEMENTARY MATERIAL

Appendix A: Multiparticle entanglement

When considering a multiparticle quantum system, there exist two different approaches to entanglement, one referring to a particular partition of the composite system under consideration (partition-dependent setting), and another which considers indiscriminately all the partitions with a set number of parties (partition-independent setting).

In order to characterise the possible partitions of an N -qubit system, we will employ the following notation [26] :

- the positive integer M , $1 < M \leq N$, representing the number of subsystems;
- the sequence of positive integers $\{K_\alpha\}_{\alpha=1}^M := \{K_1, K_2, \dots, K_M\}$, where a given K_α represents the number of qubits belonging to the α -th subsystem;
- the sequence of sequences of positive integers $\{Q_\alpha\}_{\alpha=1}^M$, such that $Q_\alpha = \{i_1^{(\alpha)}, i_2^{(\alpha)}, \dots, i_{K_\alpha}^{(\alpha)}\}$ with $i_j^{(\alpha)} \in \{1, \dots, N\}$ and $Q_\alpha \cap Q_{\alpha'} = \emptyset$ for $\alpha \neq \alpha'$, where a given sequence Q_α represents precisely the qubits belonging to the α -th subsystem.

In the following we will say that $\{Q_\alpha\}_{\alpha=1}^M$ identifies a generic M -partition of an N -qubit system.

The set of N -qubit separable states $\mathcal{S}_{\{Q_\alpha\}_{\alpha=1}^M}$ with respect to the M -partition $\{Q_\alpha\}_{\alpha=1}^M$ contains all, and only, states ς of the form

$$\varsigma = \sum_i p_i \tau_i^{(1)} \otimes \tau_i^{(2)} \otimes \dots \otimes \tau_i^{(M)}, \quad (\text{A1})$$

where $\{p_i\}$ forms a probability distribution and $\tau_i^{(\alpha)}$ are arbitrary states of the α -th subsystem. In other words, any $\{Q_\alpha\}_{\alpha=1}^M$ -separable state can be written as a convex combination of product states that are all factorised with respect to the same partition $\{Q_\alpha\}_{\alpha=1}^M$. On the other hand, the set of N -qubit M -separable states \mathcal{S}_M contains all, and only, states that can be written as convex combinations of product states, each of which is factorised with respect to an M -partition that need not be the same. One can easily see that the set of M -separable states is the convex hull of the union of all the sets of $\{Q_\alpha\}_{\alpha=1}^M$ -separable states obtained by considering all the possible M -partitions $\{Q_\alpha\}_{\alpha=1}^M$.

Any valid measure of multiparticle entanglement must be zero on the relevant set of separable states and monotonically non-increasing under local operations and classical communication (LOCC). In the partition-dependent setting, a LOCC with respect to a particular $\{Q_\alpha\}_{\alpha=1}^M$ -partition amounts to allowing each of the M parties to perform local operations on their qubits, and communicate with any other party via a classical channel [5]. Conversely, in the partition-independent setting, one considers operations that are LOCC with respect to

all of the M -partitions, which can be shown to be all and only the single-particle LOCC. A convex combination of single-particle local unitaries acting on a state ϱ , given by

$$\sum_i p_i U_i^{(1)} \otimes U_i^{(2)} \otimes \dots \otimes U_i^{(N)} \varrho U_i^{(1)\dagger} \otimes U_i^{(2)\dagger} \otimes \dots \otimes U_i^{(N)\dagger}, \quad (\text{A2})$$

is a particular type of single-particle LOCC (requiring only one-way communication). It can be physically achieved by allowing one of the subsystems α to randomly select a local unitary $U_i^{(\alpha)}$ by using the probability distribution $\{p_i\}$ and then to communicate the result to all the other subsystems.

One can also impose that a measure of N -particle entanglement is convex under convex combinations of quantum states, i.e.

$$\begin{aligned} E_{\{Q_\alpha\}_{\alpha=1}^M}(\varrho\varrho + (1-q)\varrho') &\leq qE_{\{Q_\alpha\}_{\alpha=1}^M}(\varrho) + (1-q)E_{\{Q_\alpha\}_{\alpha=1}^M}(\varrho'), \\ E_M(\varrho\varrho + (1-q)\varrho') &\leq qE_M(\varrho) + (1-q)E_M(\varrho') \end{aligned} \quad (\text{A3})$$

for some probability q and quantum states ϱ and ϱ' , which ensures that classical mixing of quantum states cannot lead to an increasing of entanglement. Any measure obeying these properties is referred to as a convex entanglement monotone. In this work we adopt geometric measures of multiparticle entanglement, defined in terms of the distance to the relevant set of separable states. For a given distance D , generic distance-based measures of the multiparticle entanglement of an N -qubit state ϱ , quantifying how much ϱ is not $\{Q_\alpha\}_{\alpha=1}^M$ -separable (resp., M -separable), are given by, respectively,

$$E_{\{Q_\alpha\}_{\alpha=1}^M}^D(\varrho) \equiv \inf_{\varsigma \in \mathcal{S}_{\{Q_\alpha\}_{\alpha=1}^M}} D(\varrho, \varsigma), \quad (\text{A4})$$

$$E_M^D(\varrho) \equiv \inf_{\varsigma \in \mathcal{S}_M} D(\varrho, \varsigma), \quad (\text{A5})$$

where Eq. (A4) refers to the partition-dependent setting, and Eq. (A5) to the partition-independent one. It is sufficient for the distance D to obey contractivity and joint convexity (see Methods in the main text) for $E_{\{Q_\alpha\}_{\alpha=1}^M}^D$ and E_M^D to be convex entanglement monotones [4].

Appendix B: The set of \mathcal{M}_N^3 states

In this appendix we show some relevant properties of the subclass of N -qubit states with all maximally mixed marginals that we refer to as \mathcal{M}_N^3 states. Their matrix representation in the computational basis is the following:

$$\varpi = \frac{1}{2^N} \left(\mathbb{I}^{\otimes N} + \sum_{i=1}^3 c_i \sigma_i^{\otimes N} \right), \quad (\text{B1})$$

where \mathbb{I} is the 2×2 identity matrix, σ_i is the i -th Pauli matrix, $c_i = \text{Tr}[\varpi \sigma_i^{\otimes N}] \in [-1, 1]$ and $N > 1$. These states are denoted by the triple $\{c_1, c_2, c_3\}$.

The characterisation of the \mathcal{M}_N^3 states is manifestly different between the even and odd N case. For even N , the eigenvectors and eigenvalues are given by, respectively,

$$|\beta_i^\pm\rangle = \frac{1}{\sqrt{2}} (\mathbb{I}^{\otimes N} \pm \sigma_1^{\otimes N}) |i\rangle, \quad (\text{B2})$$

and

$$\lambda_p^\pm = \frac{1}{2^N} \left[1 \pm c_1 \pm (-1)^{N/2} (-1)^p c_2 + (-1)^p c_3 \right], \quad (\text{B3})$$

where $i \in \{1, \dots, 2^{N-1}\}$, $\{|i\rangle\}_{i=1}^{2^N}$ is the binary ordered N -qubit computational basis and finally p is the parity of $|\beta_i^\pm\rangle$ with respect to the parity operator along the z -axis $\Pi_3 = \sigma_3^{\otimes N}$, i.e.

$$\Pi_3 |\beta_i^\pm\rangle = (-1)^p |\beta_i^\pm\rangle. \quad (\text{B4})$$

In the $\{c_1, c_2, c_3\}$ -space, the set of \mathcal{M}_N^3 states with even N is represented by the tetrahedron $\mathcal{T}_{(-1)^{N/2}}$ with vertices $\{1, (-1)^{N/2}, 1\}$, $\{-1, -(-1)^{N/2}, 1\}$, $\{1, -(-1)^{N/2}, -1\}$ and $\{-1, -(-1)^{N/2}, -1\}$, as illustrated in Fig. 2(b) in the main text. This tetrahedron is constructed simply by imposing the non-negativity of the four eigenvalues (B3) of such \mathcal{M}_N^3 states.

For odd N , the eigenvectors and eigenvalues of the \mathcal{M}_N^3 states can be easily written in spherical coordinates as

$$\begin{aligned} |\alpha_i^\pm\rangle &= \cos \left[\frac{\theta}{2} + (1 \mp (-1)^p) \frac{\pi}{4} \right] |i\rangle \\ &+ (-1)^p e^{i(-1)^p(-1)^{\frac{N-1}{2}}\phi} \sin \left[\frac{\theta}{2} + (1 \mp (-1)^p) \frac{\pi}{4} \right] \sigma_1^{\otimes N} |i\rangle, \end{aligned} \quad (\text{B5})$$

and

$$\lambda_\pm = \frac{1}{2^N} (1 \pm r), \quad (\text{B6})$$

where $i \in \{1, \dots, 2^{N-1}\}$, $\{|i\rangle\}_{i=1}^{2^N}$ is again the binary ordered N -qubit computational basis, p is the parity of $|i\rangle$ with respect to the parity operator $\Pi_3 = \sigma_3^{\otimes N}$, $c_1 = r \sin \theta \cos \phi$, $c_2 = r \sin \theta \sin \phi$ and $c_3 = r \cos \theta$, with $r = \sqrt{c_1^2 + c_2^2 + c_3^2}$, $\theta \in [0, \pi]$ and $\phi \in [0, 2\pi]$.

Consequently, thanks again to the semi-positivity constraint, the set of \mathcal{M}_N^3 states with odd N is represented in the $\{c_1, c_2, c_3\}$ -space by the unit ball \mathcal{B}_1 centred into the origin, as shown in Fig. 2(c) in the main text.

Appendix C: \mathcal{M}_N^3 -ification

The following Theorem is crucial for providing a lower bound to any multiparticle entanglement monotone of any state ϱ and for analytically computing the multiparticle geometric entanglement of any \mathcal{M}_N^3 state ϖ .

Theorem C.1. *Any N -qubit state ϱ can be transformed into a corresponding \mathcal{M}_N^3 state $\varrho_{\mathcal{M}_N^3}$ through a fixed operation, Θ , that is a single-qubit LOCC and such that*

$$\Theta(\varrho) = \varrho_{\mathcal{M}_N^3} = \frac{1}{2^N} \left(\mathbb{I}^{\otimes N} + \sum_{i=1}^3 c_i \sigma_i^{\otimes N} \right), \quad (\text{C1})$$

where $c_i = \text{Tr}(\varrho \sigma_i^{\otimes N})$.

Proof The first part of the proof was sketched in the Methods section and is repeated here for completeness.

We will give the form of $\Theta(\varrho)$, show that Θ is a single-qubit LOCC, and finally prove that it transforms any N -qubit state ϱ into $\varrho_{\mathcal{M}_N^3}$.

To define $\Theta(\varrho)$, we begin by setting $2(N-1)$ single-qubit local unitaries

$$\begin{aligned} \{U_j\}_{j=1}^{2(N-1)} = & \{(\sigma_1 \otimes \sigma_1 \otimes I^{\otimes N-2}), (I \otimes \sigma_1 \otimes \sigma_1 \otimes I^{\otimes N-3}), \\ & \dots (I^{\otimes N-3} \otimes \sigma_1 \otimes \sigma_1 \otimes I), (I^{\otimes N-2} \otimes \sigma_1 \otimes \sigma_1) \\ & , (\sigma_2 \otimes \sigma_2 \otimes I^{\otimes N-2}), (I \otimes \sigma_2 \otimes \sigma_2 \otimes I^{\otimes N-3}), \\ & \dots (I^{\otimes N-3} \otimes \sigma_2 \otimes \sigma_2 \otimes I), (I^{\otimes N-2} \otimes \sigma_2 \otimes \sigma_2)\}. \end{aligned} \quad (C2)$$

Then, we fix a sequence of states $\{\varrho_0, \varrho_1, \dots, \varrho_{2(N-1)}\}$ defined by

$$\varrho_j \equiv \frac{1}{2} (\varrho_{j-1} + U_j \varrho_{j-1} U_j^\dagger) \quad (C3)$$

for $j \in \{1, 2, \dots, 2(N-1)\}$. By setting $\varrho_0 = \varrho$ and $\varrho_{2(N-1)} = \Theta(\varrho)$, we define the required LOCC channel, i.e. $\Theta(\varrho) = \frac{1}{2^{2(N-1)}} \sum_{i=1}^{2(N-1)} U'_i \varrho U'_i$ where U'_i are the following unitaries

$$\{U'_i\}_{i=1}^{2(N-1)} = \left\{ \begin{array}{c} \mathbb{I}^{\otimes N} \\ \{U_{i_1}\}_{i_1=1}^{2(N-1)} \\ \{U_{i_2} U_{i_1}\}_{i_2 > i_1=1}^{2(N-1)} \\ \dots \\ \{U_{i_{2(N-1)}} \dots U_{i_2} U_{i_1}\}_{i_{2(N-1)} > \dots > i_2 > i_1=1}^{2(N-1)} \end{array} \right\}. \quad (C4)$$

It is clear that $\{U'_i\}_{i=1}^{2(N-1)}$ are unitaries that still act locally on individual qubits. Since Θ is a convex mixture of such local unitaries, we conclude that Θ is a single-qubit LOCC.

Now we will show that $\Theta(\varrho) = \varrho_{\mathcal{M}_N^3}$. Consider the arbitrary N -qubit state ϱ written in the form

$$\varrho = \frac{1}{2^N} \sum_{i_1 i_2 \dots i_N=0}^3 R_{i_1 i_2 \dots i_N}^\varrho \sigma_{i_1} \otimes \sigma_{i_2} \dots \otimes \sigma_{i_N}, \quad (C5)$$

where the $R_{i_1 i_2 \dots i_N}^\varrho = \text{Tr}[\varrho \sigma_{i_1} \otimes \sigma_{i_2} \dots \otimes \sigma_{i_N}] \in [-1, 1]$ are the correlation tensor elements of ϱ with $\sigma_0 = \mathbb{I}$. Convex combination of two arbitrary N -qubit states ϱ and ϱ' gives

$$q\varrho + (1-q)\varrho' = \frac{1}{2^N} \sum_{i_1 i_2 \dots i_N=0}^3 R_{i_1 i_2 \dots i_N}^{q\varrho + (1-q)\varrho'} \sigma_{i_1} \otimes \sigma_{i_2} \dots \otimes \sigma_{i_N} \quad (C6)$$

where $R_{i_1 i_2 \dots i_N}^{q\varrho + (1-q)\varrho'} = qR_{i_1 i_2 \dots i_N}^\varrho + (1-q)R_{i_1 i_2 \dots i_N}^{\varrho'}$.

We will now understand the evolution of the $R_{i_1 i_2 \dots i_N}^{\varrho_j}$ for each step j in Eq. (C3). The action of U_1 on ϱ is

$$\begin{aligned} U_1 \varrho U_1^\dagger = & \frac{1}{2^N} \sum_{i_1 i_2 \dots i_N=0}^3 R_{i_1 i_2 \dots i_N}^\varrho \sigma_1 \sigma_{i_1} \sigma_1 \otimes \sigma_1 \sigma_{i_2} \sigma_1 \\ & \otimes \sigma_{i_3} \dots \otimes \sigma_{i_N}. \end{aligned} \quad (C7)$$

From $\sigma_1 \sigma_i \sigma_1 = -(-1)^{\delta_{0i} + \delta_{1i}} \sigma_i$ we have that the correlation tensor elements of $U_1 \varrho U_1^\dagger$ are $R_{i_1 i_2 \dots i_N}^{U_1 \varrho U_1^\dagger} = (-1)^{\delta_{0i_1} + \delta_{1i_1} + \delta_{0i_2} + \delta_{1i_2}} R_{i_1 i_2 \dots i_N}^\varrho$. By using Eq. (C3) and Eq. (C6), it

is clear that the $R_{i_1 i_2 \dots i_N}^{\varrho_1}$ of ϱ_1 are $R_{i_1 i_2 \dots i_N}^\varrho$ if i_1 and i_2 are (i) any combination of only 1 and 0 or (ii) any combination of only 2 and 3, and zero otherwise.

Generally, for $j \in [1, N-1]$, the $R_{i_1 i_2 \dots i_N}^{\varrho_j}$ of ϱ_j are $R_{i_1 i_2 \dots i_N}^{\varrho_{j-1}}$ if i_j and i_{j+1} are (i) any combination of only 1 and 0 or (ii) any combination of only 2 and 3, and zero otherwise. For $j \in [N, 2(N-1)]$ the conditions are analogous, where the $R_{i_1 i_2 \dots i_N}^{\varrho_j}$ of ϱ_j are $R_{i_1 i_2 \dots i_N}^{\varrho_{j-1}}$ if i_j and i_{j+1} are (i) any combination of only 2 and 0 or (ii) any combination of only 1 and 3, and zero otherwise. For the final state $\varrho_{2(N-1)}$, the only nonzero $R_{i_1 i_2 \dots i_N}^{\varrho_{2(N-1)}}$ are those for which $\{i_1 i_2 \dots i_N\}$ consists of only 0, 1, 2, or 3, and that for these elements $R_{i_1 i_2 \dots i_N}^{\varrho_{2(N-1)}} = R_{i_1 i_2 \dots i_N}^\varrho$. Therefore

$$\begin{aligned} \Theta(\varrho) = \varrho_{2(N-1)} &= \frac{1}{2^N} \sum_{i=0}^3 R_{ii \dots i}^\varrho \sigma_i \otimes \sigma_i \dots \otimes \sigma_i \\ &\equiv \frac{1}{2^N} \left(\mathbb{I}^{\otimes N} + \sum_{i=1}^3 c_i \sigma_i^{\otimes N} \right) = \varrho_{\mathcal{M}_N^3} \end{aligned} \quad (C8)$$

where we have used $R_{ii \dots i}^\varrho = \text{Tr}(\varrho \sigma_i^{\otimes N}) \equiv c_i$ for $i \in \{1, 2, 3\}$ and $R_{00 \dots 0}^\varrho = \text{Tr}(\varrho) = 1$. ■

Herein, we will refer to $\varrho_{\mathcal{M}_N^3} = \Theta(\varrho)$ as the \mathcal{M}_N^3 -fication of the state ϱ . Theorem C.1 has two major implications. The first implication applies to any multiparticle entanglement monotone, be it partition-dependent or independent. We have that

$$E_{\{\mathcal{Q}_\alpha\}_{\alpha=1}^M}(\varrho_{\mathcal{M}_N^3}) = E_{\{\mathcal{Q}_\alpha\}_{\alpha=1}^M}(\Theta(\varrho)) \leq E_{\{\mathcal{Q}_\alpha\}_{\alpha=1}^M}(\varrho), \quad (C9)$$

$$E_M(\varrho_{\mathcal{M}_N^3}) = E_M(\Theta(\varrho)) \leq E_M(\varrho), \quad (C10)$$

where in the first equality we use $\varrho_{\mathcal{M}_N^3} = \Theta(\varrho)$ and in the inequality we use the monotonicity under single-qubit LOCC of any measure of multiparticle entanglement and the fact that Θ is a single-qubit LOCC. In other words, the multiparticle entanglement of the \mathcal{M}_N^3 -fication $\varrho_{\mathcal{M}_N^3}$ of any state ϱ provides us with a lower bound of the multiparticle entanglement of ϱ .

The second implication applies specifically to distance-based measures of multiparticle entanglement, although regardless of whether such a measure is partition-dependent or independent. We have that, for any \mathcal{M}_N^3 state ϖ and any separable state ς ,

$$D(\varpi, \varsigma_{\mathcal{M}_N^3}) = D(\Theta(\varpi), \Theta(\varsigma)) \leq D(\varpi, \varsigma), \quad (C11)$$

where in the first equality we use the invariance of any \mathcal{M}_N^3 state through Θ and that $\Theta(\varsigma) \equiv \varsigma_{\mathcal{M}_N^3}$ is the \mathcal{M}_N^3 -fication of ς , and in the inequality we use the contractivity of the distance through any completely positive trace-preserving channel. Moreover, the \mathcal{M}_N^3 -fication $\varsigma_{\mathcal{M}_N^3}$ of any separable state ς , regardless of whether ς is $\{\mathcal{Q}_\alpha\}_{\alpha=1}^M$ -separable or M -separable, is a separable \mathcal{M}_N^3 state of the same kind as ς , since Θ is a single-qubit LOCC and thus leaves any set of separable states invariant. Therefore, both the sets $\mathcal{S}_{\{\mathcal{Q}_\alpha\}_{\alpha=1}^M}^{\mathcal{M}_N^3}$ and $\mathcal{S}_M^{\mathcal{M}_N^3}$ of, respectively, $\{\mathcal{Q}_\alpha\}_{\alpha=1}^M$ -separable and M -separable \mathcal{M}_N^3 states will be crucial to identify (see Appendix D), since they allow us to

use Eq. (C11) to say that for any distance-based measure of multiparticle entanglement of an \mathcal{M}_N^3 state ϖ ,

$$\begin{aligned} E_{\{Q_\alpha\}_{\alpha=1}^M}^D(\varpi) &\equiv \inf_{\varsigma \in \mathcal{S}_{\{Q_\alpha\}_{\alpha=1}^M}} D(\varpi, \varsigma) = \inf_{\substack{\varsigma_{\mathcal{M}_N^3} \in \mathcal{S}_{\{Q_\alpha\}_{\alpha=1}^M}^{\mathcal{M}_N^3} \\ \varsigma_{\mathcal{M}_N^3} \in \mathcal{S}_{\{Q_\alpha\}_{\alpha=1}^M}^{\mathcal{M}_N^3}}} D(\varpi, \varsigma_{\mathcal{M}_N^3}), \\ E_M^D(\varpi) &\equiv \inf_{\varsigma \in \mathcal{S}_M} D(\varpi, \varsigma) = \inf_{\varsigma_{\mathcal{M}_N^3} \in \mathcal{S}_M^{\mathcal{M}_N^3}} D(\varpi, \varsigma_{\mathcal{M}_N^3}), \end{aligned} \quad (\text{C12})$$

i.e. that one of the closest $\{Q_\alpha\}_{\alpha=1}^M$ -separable (resp., M -separable) states ς_ϖ to an \mathcal{M}_N^3 state ϖ is itself an \mathcal{M}_N^3 state. We now formalise these two results as corollaries.

Corollary C.1. *For any N -qubit state ϱ , the multiparticle entanglement of the corresponding \mathcal{M}_N^3 -fied state $\varrho_{\mathcal{M}_N^3}$ is always less than or equal to the multiparticle entanglement of ϱ , i.e.*

$$E_{\{Q_\alpha\}_{\alpha=1}^M}(\varrho_{\mathcal{M}_N^3}) \leq E_{\{Q_\alpha\}_{\alpha=1}^M}(\varrho), \quad (\text{C13})$$

$$E_M(\varrho_{\mathcal{M}_N^3}) \leq E_M(\varrho), \quad (\text{C14})$$

for any $\{Q_\alpha\}_{\alpha=1}^M$ -partition of the N -qubit system and any $2 \leq M \leq N$.

Corollary C.2. *For any contractive distance D and any \mathcal{M}_N^3 state ϖ , one of the closest $\{Q_\alpha\}_{\alpha=1}^M$ -separable (resp., M -separable) states ς_ϖ to ϖ is itself an \mathcal{M}_N^3 state, i.e.*

$$\varsigma_\varpi = \frac{1}{2^N} \left(\mathbb{I}^{\otimes N} + \sum_i s_i \sigma_i^{\otimes N} \right), \quad (\text{C15})$$

for any $\{Q_\alpha\}_{\alpha=1}^M$ -partition of the N -qubit system and any $2 \leq M \leq N$.

Theorem C.1 allows for another result which will be useful to characterise the set of separable \mathcal{M}_N^3 states.

Corollary C.3. *The set of the triples $\{c_1, c_2, c_3\}$, with $c_i = \text{Tr}(\varrho \sigma_i^{\otimes N})$, obtained by considering any possible N -qubit state ϱ is*

- the unit ball \mathcal{B}_1 , when N is odd;
- the tetrahedron $\mathcal{T}_{(-1)^{N/2}}$, when N is even.

This is because the set of \mathcal{M}_N^3 -ficiations of all the states coincides exactly with the set of \mathcal{M}_N^3 states. Indeed, the \mathcal{M}_N^3 -fication channel Θ makes the entire set of states collapse into the set of \mathcal{M}_N^3 states, whereas it leaves the set of \mathcal{M}_N^3 states invariant. Herein, we shall refer to the triple $\{c_1, c_2, c_3\}$, with $c_i = \text{Tr}(\varrho \sigma_i^{\otimes N})$, as the Pauli correlation vector corresponding to the state ϱ .

Appendix D: The set of separable \mathcal{M}_N^3 states

We are now ready to characterise the sets $\mathcal{S}_{\{Q_\alpha\}_{\alpha=1}^M}^{\mathcal{M}_N^3}$ and $\mathcal{S}_M^{\mathcal{M}_N^3}$ of, respectively, $\{Q_\alpha\}_{\alpha=1}^M$ -separable and M -separable \mathcal{M}_N^3 states. The first ingredient is to note that $\mathcal{S}_{\{Q_\alpha\}_{\alpha=1}^M}^{\mathcal{M}_N^3}$ coincides

exactly with the set $\Theta[\mathcal{S}_{\{Q_\alpha\}_{\alpha=1}^M}]$ of the \mathcal{M}_N^3 -ficiations of any $\{Q_\alpha\}_{\alpha=1}^M$ -separable state. Furthermore, we note that since any \mathcal{M}_N^3 state is invariant under any permutation of the N qubits, then the set of $\{Q_\alpha\}_{\alpha=1}^M$ -separable \mathcal{M}_N^3 states $\mathcal{S}_{\{Q_\alpha\}_{\alpha=1}^M}^{\mathcal{M}_N^3}$ does not depend on which qubits belong to each of the subsystems. Therefore we need only to specify the cardinalities $\{K_\alpha\}_{\alpha=1}^M$ to completely characterise $\mathcal{S}_{\{Q_\alpha\}_{\alpha=1}^M}^{\mathcal{M}_N^3}$, and we will herein refer to the latter as the set of $\{K_\alpha\}_{\alpha=1}^M$ -separable \mathcal{M}_N^3 states $\mathcal{S}_{\{K_\alpha\}_{\alpha=1}^M}^{\mathcal{M}_N^3}$.

Theorem D.1. *For any N , the set of separable \mathcal{M}_N^3 states $\mathcal{S}_{\{K_\alpha\}_{\alpha=1}^M}^{\mathcal{M}_N^3}$ is either*

- the set of all \mathcal{M}_N^3 states, for any allowed $\{K_\alpha\}_{\alpha=1}^M$ partition such that K_α is odd for at most one value of α ;
- the set of \mathcal{M}_N^3 states represented in the $\{c_1, c_2, c_3\}$ -space by the unit octahedron \mathcal{O}_1 with vertices $\{\pm 1, 0, 0\}$, $\{0, \pm 1, 0\}$ and $\{0, 0, \pm 1\}$, for any allowed $\{K_\alpha\}_{\alpha=1}^M$ partition such that K_α is odd for more than one value of α .

Proof

In order to characterise the set of $\{K_\alpha\}_{\alpha=1}^M$ -separable \mathcal{M}_N^3 states, $\mathcal{S}_{\{K_\alpha\}_{\alpha=1}^M}^{\mathcal{M}_N^3}$, we simply need to identify its representation in the $\{c_1, c_2, c_3\}$ -space. Since $\mathcal{S}_{\{K_\alpha\}_{\alpha=1}^M}^{\mathcal{M}_N^3} = \Theta[\mathcal{S}_{\{Q_\alpha\}_{\alpha=1}^M}]$, we know that such a representation is the set of Pauli correlation vectors corresponding to all the elements of $\mathcal{S}_{\{Q_\alpha\}_{\alpha=1}^M}$.

Due to Eq. (A1), the Pauli correlation vector of any $\varsigma \in \mathcal{S}_{\{Q_\alpha\}_{\alpha=1}^M}$ is given by

$$\begin{aligned} s_j &= \text{Tr}(\varrho \sigma_j^{\otimes N}) = \text{Tr} \left[\left(\sum_i p_i \tau_i^{(1)} \otimes \tau_i^{(2)} \otimes \dots \otimes \tau_i^{(M)} \right) \sigma_j^{\otimes N} \right] \\ &= \sum_i p_i \text{Tr} \left[\tau_i^{(1)} \sigma_j^{\otimes K_1} \otimes \tau_i^{(2)} \sigma_j^{\otimes K_2} \otimes \dots \otimes \tau_i^{(M)} \sigma_j^{\otimes K_M} \right] \\ &= \sum_i p_i \prod_{\alpha=1}^M \text{Tr} \left(\tau_i^{(\alpha)} \sigma_j^{\otimes K_\alpha} \right) = \sum_i p_i \prod_{\alpha=1}^M c_{i,j}^{(\alpha)} \end{aligned} \quad (\text{D1})$$

where in the final equality we denote $c_{i,j}^{(\alpha)} = \text{Tr}(\tau_i^{(\alpha)} \sigma_j^{\otimes K_\alpha})$ as the j -th component of the Pauli correlation vector $\vec{c}_i^{(\alpha)} = \{c_{i,1}^{(\alpha)}, c_{i,2}^{(\alpha)}, c_{i,3}^{(\alpha)}\}$ corresponding to the arbitrary state $\tau_i^{(\alpha)}$ of subsystem α . Eq. (D1) can be simplified further by introducing the Hadamard product as the componentwise multiplication of vectors, i.e. for $\vec{u} = \{u_1, u_2, u_3\}$ and $\vec{v} = \{v_1, v_2, v_3\}$ the Hadamard product is $\vec{u} \circ \vec{v} = \{u_1 v_1, u_2 v_2, u_3 v_3\}$. Using the Hadamard product gives Eq. (D1) as

$$\vec{s} = \sum_i p_i \vec{c}_i^{(1)} \circ \vec{c}_i^{(2)} \circ \dots \circ \vec{c}_i^{(M)}, \quad (\text{D2})$$

i.e., that the Pauli correlation vector of any $\{Q_\alpha\}_{\alpha=1}^M$ -separable state is a convex combination of Hadamard products of Pauli correlation vectors corresponding to subsystem states. Due to Corollary C.3, we know that $\vec{c}_i^{(\alpha)} \in \mathcal{B}_1$ when K_α is odd and

$\vec{c}_i^{(\alpha)} \in \mathcal{T}_{(-1)^{K_\alpha/2}}$ when K_α is even, and so $\mathcal{S}_{\{K_\alpha\}_{\alpha=1}^M}^{\mathcal{M}_N^3}$ is represented by the following set

$$\mathcal{S}_{\{K_\alpha\}_{\alpha=1}^M}^{\mathcal{M}_N^3} = \text{conv} \left(A^{(1)} \circ A^{(2)} \circ \dots \circ A^{(M)} \right), \quad (\text{D3})$$

with

$$A^{(\alpha)} = \begin{cases} \mathcal{B}_1 & \text{if } K_\alpha \text{ is odd,} \\ \mathcal{T}_{(-1)^{K_\alpha/2}} & \text{if } K_\alpha \text{ is even,} \end{cases} \quad (\text{D4})$$

where we define the Hadamard product between any two sets A and B as $A \circ B = \{\vec{a} \circ \vec{b} \mid \vec{a} \in A, \vec{b} \in B\}$ and the convex hull $\text{conv}(A)$ is the set of all possible convex combinations of elements in A . The commutativity and associativity of the Hadamard product allow us to rearrange the ordering in Eq. (D3) in the following way

$$\mathcal{S}_{\{K_\alpha\}_{\alpha=1}^M}^{\mathcal{M}_N^3} = \text{conv} \left[\left(\bigcap_{\mu: K_\mu \text{ even}} \mathcal{T}_{(-1)^{K_\mu/2}} \right) \circ \left(\bigcap_{\nu: K_\nu \text{ odd}} \mathcal{B}_1 \right) \right], \quad (\text{D5})$$

where $\bigcap_{\alpha=1}^n A^{(\alpha)} = A^{(1)} \circ A^{(2)} \circ \dots \circ A^{(n)}$.

By writing any vector in $\mathcal{T}_{\pm 1}$ as a convex combination of the vertices of $\mathcal{T}_{\pm 1}$, one can easily show that

$$\begin{aligned} \mathcal{T}_{-1} \circ \mathcal{T}_{-1} &= \mathcal{T}_1, \\ \mathcal{T}_1 \circ \mathcal{T}_1 &= \mathcal{T}_1, \\ \mathcal{T}_1 \circ \mathcal{T}_{-1} &= \mathcal{T}_{-1}, \end{aligned} \quad (\text{D6})$$

so that

$$\bigcap_{\mu: K_\mu \text{ even}} \mathcal{T}_{(-1)^{K_\mu/2}} = \mathcal{T}_{(-1)^{\mathcal{M}_-}}, \quad (\text{D7})$$

where \mathcal{M}_- is the number of K_μ with odd $K_\mu/2$. Similarly, one can see that

$$\mathcal{T}_{\pm 1} \circ \mathcal{B}_1 = \mathcal{B}_1. \quad (\text{D8})$$

Finally, we have that

$$\text{conv} \left(\bigcap_{i=1}^n \mathcal{B}_1 \right) = \mathcal{O}_1 \quad \forall n \geq 2. \quad (\text{D9})$$

Indeed, since $\{\{\pm 1, 0, 0\}, \{0, \pm 1, 0\}, \{0, 0, \pm 1\}\} \subset \bigcap_{i=1}^n \mathcal{B}_1$ and $\text{conv} \{ \{\pm 1, 0, 0\}, \{0, \pm 1, 0\}, \{0, 0, \pm 1\} \} = \mathcal{O}_1$, we know that $\mathcal{O}_1 \subseteq \text{conv} \left(\bigcap_{i=1}^n \mathcal{B}_1 \right)$. Now we will show that $\mathcal{O}_1 \supseteq \text{conv} \left(\bigcap_{i=1}^n \mathcal{B}_1 \right)$. To do so, it is sufficient to see that

$$\vec{b} \circ \vec{b}' \in \mathcal{O}_1 \quad (\text{D10})$$

for any $\vec{b}, \vec{b}' \in \mathcal{B}_1$, which trivially implies that $\bigcap_{i=1}^n \mathcal{B}_1 \subseteq \mathcal{O}_1$, and so $\text{conv} \left(\bigcap_{i=1}^n \mathcal{B}_1 \right) \subseteq \text{conv}(\mathcal{O}_1) = \mathcal{O}_1$. Equation (D10) holds since

$$\begin{aligned} |b_1 b'_1| + |b_2 b'_2| + |b_3 b'_3| &= |b_1| |b'_1| + |b_2| |b'_2| + |b_3| |b'_3| \\ &= \vec{n} \cdot \vec{n}' = \|\vec{n}\| \|\vec{n}'\| \cos \theta \leq 1, \end{aligned} \quad (\text{D11})$$

where we define $\vec{n} = \{|b_1|, |b_2|, |b_3|\}$ and $\vec{n}' = \{|b'_1|, |b'_2|, |b'_3|\}$, respectively, as the vectors corresponding to \vec{b} and \vec{b}' in the positive octant of the unit ball, and θ as the angle between these vectors.

Now, due to Eqs. (D5), (D7), (D8) and (D9), and the fact that $\text{conv}(A) = A$ for any convex set A , we identify four cases:

1. if K_α is even for any α then

$$\begin{aligned} \mathcal{S}_{\{K_\alpha\}_{\alpha=1}^M}^{\mathcal{M}_N^3} &= \text{conv} \left(\bigcap_{\mu: K_\mu \text{ even}} \mathcal{T}_{(-1)^{K_\mu/2}} \right) \\ &= \text{conv} \left(\mathcal{T}_{(-1)^{\mathcal{M}_-}} \right) \\ &= \mathcal{T}_{(-1)^{\mathcal{M}_-}}, \end{aligned} \quad (\text{D12})$$

where \mathcal{M}_- is the number of K_μ with odd $K_\mu/2$;

2. if K_α is odd for just one value of α then

$$\begin{aligned} \mathcal{S}_{\{K_\alpha\}_{\alpha=1}^M}^{\mathcal{M}_N^3} &= \text{conv} \left[\left(\bigcap_{\mu: K_\mu \text{ even}} \mathcal{T}_{(-1)^{K_\mu/2}} \right) \circ \mathcal{B}_1 \right] \\ &= \text{conv} \left(\mathcal{T}_{\pm 1} \circ \mathcal{B}_1 \right) \\ &= \mathcal{B}_1; \end{aligned} \quad (\text{D13})$$

3. if K_α is odd for all values of α then

$$\begin{aligned} \mathcal{S}_{\{K_\alpha\}_{\alpha=1}^M}^{\mathcal{M}_N^3} &= \text{conv} \left(\bigcap_{\nu: K_\nu \text{ odd}} \mathcal{B}_1 \right) \\ &= \mathcal{O}_1; \end{aligned} \quad (\text{D14})$$

4. otherwise,

$$\begin{aligned} \mathcal{S}_{\{K_\alpha\}_{\alpha=1}^M}^{\mathcal{M}_N^3} &= \text{conv} \left[\left(\bigcap_{\mu: K_\mu \text{ even}} \mathcal{T}_{(-1)^{K_\mu/2}} \right) \circ \left(\bigcap_{\nu: K_\nu \text{ odd}} \mathcal{B}_1 \right) \right] \\ &= \text{conv} \left[\mathcal{T}_{\pm 1} \circ \left(\bigcap_{\nu: K_\nu \text{ odd}} \mathcal{B}_1 \right) \right] \\ &= \text{conv} \left[\mathcal{T}_{\pm 1} \circ \mathcal{B}_1 \circ \dots \circ \mathcal{B}_1 \right] \\ &= \text{conv} \left(\bigcap_{\nu: K_\nu \text{ odd}} \mathcal{B}_1 \right) \\ &= \mathcal{O}_1. \end{aligned} \quad (\text{D15})$$

For any even N -qubit system, only a $\{K_\alpha\}_{\alpha=1}^M$ partitioning within cases 1, 3 and 4 may be realised. In case 1, i.e. when K_α is even for any α , we have $\mathcal{S}_{\{K_\alpha\}_{\alpha=1}^M}^{\mathcal{M}_N^3} = \mathcal{T}_{(-1)^{\mathcal{M}_-}}$, where \mathcal{M}_- is the number of K_α with odd $K_\alpha/2$. However, one can simply see that $(-1)^{\mathcal{M}_-} = (-1)^{N/2}$, and thus $\mathcal{S}_{\{K_\alpha\}_{\alpha=1}^M}^{\mathcal{M}_N^3}$ is the set $\mathcal{T}_{(-1)^{N/2}}$ of all \mathcal{M}_N^3 states. Otherwise, in cases 3 and 4, we have $\mathcal{S}_{\{K_\alpha\}_{\alpha=1}^M}^{\mathcal{M}_N^3} = \mathcal{O}_1$.

For any odd N -qubit system, only a $\{K_\alpha\}_{\alpha=1}^M$ partitioning within cases 2, 3 and 4 may be realised. In case 2, i.e. when K_α is odd for only one α , we have $\mathcal{S}_{\{K_\alpha\}_{\alpha=1}^M}^{\mathcal{M}_N^3} = \mathcal{B}_1$, and thus $\mathcal{S}_{\{K_\alpha\}_{\alpha=1}^M}^{\mathcal{M}_N^3}$ is the set \mathcal{B}_1 of all \mathcal{M}_N^3 states. Otherwise, in cases 3 and 4, we have $\mathcal{S}_{\{K_\alpha\}_{\alpha=1}^M}^{\mathcal{M}_N^3} = \mathcal{O}_1$.

■

By identifying the set of separable \mathcal{M}_N^3 states $\mathcal{S}_{\{Q_\alpha\}_{\alpha=1}^M}^{\mathcal{M}_N^3}$, Theorem D.1 implies the following corollary.

Corollary D.1. *For any multiparticle entanglement monotone $E_{\{Q_\alpha\}_{\alpha=1}^M}$ and any \mathcal{M}_N^3 state ϖ partitioned along any given $\{Q_\alpha\}_{\alpha=1}^M$ -partition, $E_{\{Q_\alpha\}_{\alpha=1}^M}(\varpi) = 0$ if*

1. K_α is odd for at most one value of α ;
2. K_α is odd for more than one value of α and $|c_1| + |c_2| + |c_3| \leq 1$ for $c_i = \text{Tr}(\varpi \sigma_i^{\otimes N})$.

Now we are ready to characterise also the set of M -separable \mathcal{M}_N^3 states $\mathcal{S}_M^{\mathcal{M}_N^3}$. Indeed we know that $\mathcal{S}_M^{\mathcal{M}_N^3}$ is just the convex hull of the union of all the sets of $\{Q_\alpha\}_{\alpha=1}^M$ -separable \mathcal{M}_N^3 states $\mathcal{S}_{\{Q_\alpha\}_{\alpha=1}^M}^{\mathcal{M}_N^3}$ obtained by considering all the possible M -partitions $\{Q_\alpha\}_{\alpha=1}^M$. Furthermore, one can easily see that for any $M \leq \lceil N/2 \rceil$ one can always find an M -partition $\{Q_\alpha\}_{\alpha=1}^M$ such that K_α is odd for at most one value of α and thus $\mathcal{S}_{\{Q_\alpha\}_{\alpha=1}^M}^{\mathcal{M}_N^3} = \mathcal{M}_N^3$, whereas for any $M > \lceil N/2 \rceil$ this is impossible and thus $\mathcal{S}_{\{Q_\alpha\}_{\alpha=1}^M}^{\mathcal{M}_N^3} = O_1$ for any possible M -partition $\{Q_\alpha\}_{\alpha=1}^M$. This immediately implies the following two Corollaries.

Corollary D.2. *For any N , the set of M -separable \mathcal{M}_N^3 states $\mathcal{S}_M^{\mathcal{M}_N^3}$ is either*

- the set of all \mathcal{M}_N^3 states, for any $M \leq \lceil N/2 \rceil$;
- the set of \mathcal{M}_N^3 states represented in the $\{c_1, c_2, c_3\}$ -space by the unit octahedron O_1 with vertices $\{\pm 1, 0, 0\}$, $\{0, \pm 1, 0\}$ and $\{0, 0, \pm 1\}$, for any $M > \lceil N/2 \rceil$.

Corollary D.3. *For any multiparticle entanglement monotone E_M and any \mathcal{M}_N^3 state ϖ , $E_M(\varpi) = 0$ if*

1. $M \leq \lceil N/2 \rceil$;
2. $M > \lceil N/2 \rceil$ and $|c_1| + |c_2| + |c_3| \leq 1$ for $c_i = \text{Tr}(\varpi \sigma_i^{\otimes N})$.

Appendix E: Multiparticle entanglement of \mathcal{M}_N^3 states

We now provide the analytical expressions for both the partition-dependent and partition-independent geometric measures of multiparticle entanglement $E_{\{Q_\alpha\}_{\alpha=1}^M}^D(\varpi)$ and $E_M^D(\varpi)$ of any \mathcal{M}_N^3 state ϖ . Within the partition-dependent setting we will restrict to any nontrivial partition $\{K'_\alpha\}_{\alpha=1}^M$, i.e. such that K'_α is odd for at least two values of α , whereas within the partition-independent setting we will restrict to any nontrivial number of parties M' , i.e. such that $M' > \lceil N/2 \rceil$. According to Appendix C and D, in both cases we simply need to find the minimal distance from ϖ to the set of \mathcal{M}_N^3 states inside the unit octahedron O_1 . In the even N case, the closest state is the same for any convex and contractive distance (note that every jointly convex distance is convex), while in the odd N case this is not true.

1. Even N case

For even N , both the $\{K'_\alpha\}_{\alpha=1}^M$ - and M' -inseparable \mathcal{M}_N^3 states belong to the four corners obtained by removing the unit octahedron O_1 from the whole tetrahedron $\mathcal{T}_{(-1)^{N/2}}$ of \mathcal{M}_N^3 states. In the following we will focus only on the corner containing the vertex $\{-1, (-1)^{N/2}, -1\}$, since all the \mathcal{M}_N^3 states belonging to the other three corners can be obtained from this by simply applying a single-qubit local unitary $\sigma_i \otimes \mathbb{I}^{\otimes N-1}$, $i \in \{1, 2, 3\}$, under which any sort of multiparticle entanglement is invariant.

In order to characterise all the \mathcal{M}_N^3 states with even N belonging to the $\{-1, (-1)^{N/2}, -1\}$ -corner, it will be convenient to move from the coordinate system $\{c_1, c_2, c_3\}$ to a new coordinate system (p, q, h) , where we assign the coordinates $(\frac{1}{3}, \frac{1}{3}, 1)$ to the vertex $\{-1, (-1)^{N/2}, -1\}$ and the coordinates

$$p = \frac{1 + c_1 - (-1)^{N/2}c_2 - c_3}{3 + c_1 - (-1)^{N/2}c_2 + c_3}, \quad (\text{E1})$$

$$q = \frac{1 + c_1 + (-1)^{N/2}c_2 + c_3}{3 + c_1 - (-1)^{N/2}c_2 + c_3}, \quad (\text{E2})$$

$$h = (-1 - (c_1 - (-1)^{N/2}c_2 + c_3))/2, \quad (\text{E3})$$

to any other point in the corner. In order to avoid confusion between the above two coordinate systems, we will denote an \mathcal{M}_N^3 state ϖ with curly brackets when representing it in the $\{c_1, c_2, c_3\}$ coordinate system, whereas we will denote ϖ with round brackets when representing it in the (p, q, h) coordinate system. Specifically, the \mathcal{M}_N^3 states represented by the triples (p, q, h) , with a fixed value of $h \in [0, 1[$, correspond in the $\{c_1, c_2, c_3\}$ -space to all, and only, the \mathcal{M}_N^3 states belonging to the triangle with the following vertices:

$$\begin{aligned} V_1(h) &= \{-h, (-1)^{N/2}h, -1\}, \\ V_2(h) &= \{-h, (-1)^{N/2}, -h\}, \\ V_3(h) &= \{-1, (-1)^{N/2}h, -h\}, \end{aligned} \quad (\text{E4})$$

in such a way that

$$(p, q, h) = pV_1(h) + qV_2(h) + (1 - p - q)V_3(h). \quad (\text{E5})$$

These triangles corresponding to constant values of h will play a crucial role, as they represent the sets of \mathcal{M}_N^3 states with constant $\{K'_\alpha\}_{\alpha=1}^M$ - and M' -inseparable multiparticle entanglement for even N . In particular, for $h = 0$ we get one of the faces of the octahedron of $\{K'_\alpha\}_{\alpha=1}^M$ - and M' -separable states, whereas with increasing h , we will prove that both the $\{K'_\alpha\}_{\alpha=1}^M$ - and M' -inseparable multiparticle entanglement of the \mathcal{M}_N^3 states belonging to the corresponding triangle will increase monotonically. We will now show that the $\{K'_\alpha\}_{\alpha=1}^M$ -separable (resp., M' -separable) state represented by the triple $(p, q, 0)$ is one of the closest $\{K'_\alpha\}_{\alpha=1}^M$ -separable (resp., M' -separable) states to the \mathcal{M}_N^3 state (p, q, h) .

Lemma E.1. *For every even N , according to any convex and contractive distance, one of the closest $\{K'_\alpha\}_{\alpha=1}^M$ -separable (resp., M' -separable) states ς_ϖ to any \mathcal{M}_N^3 state ϖ belonging*

to the $\{-1, (-1)^{N/2}, -1\}$ -corner is always an \mathcal{M}_N^3 state of the form $(p', q', 0)$ for some $p', q' \in [0, 1]$, $p' + q' \leq 1$.

Proof. Let ϖ and ς be, respectively, any \mathcal{M}_N^3 state belonging to the $\{-1, (-1)^{N/2}, -1\}$ -corner and any $\{K'_\alpha\}_{\alpha=1}^M$ -separable \mathcal{M}_N^3 state, i.e. any \mathcal{M}_N^3 state contained in the unit octahedron O_1 . There will always be a $\{K'_\alpha\}_{\alpha=1}^M$ -separable \mathcal{M}_N^3 state ς' , belonging to the octahedron face whose vertices are $V_1(0)$, $V_2(0)$, and $V_3(0)$ given in Eqs. (E4), such that $\varsigma' = \lambda\varpi + (1 - \lambda)\varsigma$ for some $\lambda \in [0, 1]$. Now, for any convex distance, the following holds

$$\begin{aligned} D(\varpi, \varsigma') & \quad (E6) \\ &= D(\varpi, \lambda\varpi + (1 - \lambda)\varsigma) \\ &\leq \lambda D(\varpi, \varpi) + (1 - \lambda)D(\varpi, \varsigma) \\ &= (1 - \lambda)D(\varpi, \varsigma) \\ &\leq D(\varpi, \varsigma). \end{aligned}$$

As one of the closest $\{K'_\alpha\}_{\alpha=1}^M$ -separable states ς_ϖ to any \mathcal{M}_N^3 state ϖ is always a $\{K'_\alpha\}_{\alpha=1}^M$ -separable \mathcal{M}_N^3 state, then the above inequality implies that, for any \mathcal{M}_N^3 state ϖ belonging to the $\{-1, (-1)^{N/2}, -1\}$ -corner, ς_ϖ always belongs to the triangle with vertices $V_1(0)$, $V_2(0)$, and $V_3(0)$ i.e. $\varsigma_\varpi = (p', q', 0)$ for some $p', q' \in [0, 1]$, $p' + q' \leq 1$. Exactly the same proof holds when substituting $\{K'_\alpha\}_{\alpha=1}^M$ -separability with M' -separability. \blacksquare

Lemma E.2. For every even N , any contractive distance satisfies the following translational invariance property:

$$D((p, q, h), (p, q, 0)) = D\left(\left(\frac{1}{3}, \frac{1}{3}, h\right), \left(\frac{1}{3}, \frac{1}{3}, 0\right)\right), \quad (E7)$$

for any $p, q \in [0, 1]$ with $p + q \leq 1$ and $h \in [0, 1]$.

Proof. First of all, by considering the following single-qubit LOCC,

$$\Lambda_{\{p, q\}}(\varrho) = p\varrho + qU_1\varrho U_1^\dagger + (1 - p - q)U_2\varrho U_2^\dagger \quad (E8)$$

where $p, q \in [0, 1]$, $p + q \leq 1$ and

$$U_1 = S_2^{\otimes N} S_1^{\otimes N} F_N, \quad (E9)$$

$$U_2 = S_1^{\otimes N} F_N S_2^{\otimes N}, \quad (E10)$$

with $S_i = \frac{1}{\sqrt{2}}(\mathbb{I} + i\sigma_i)$ and $F_N = \sigma_1^{\otimes(N/2+1)} \otimes \mathbb{I}^{\otimes(N/2-1)}$, we have the following inequality,

$$\begin{aligned} & D\left(\left(\frac{1}{3}, \frac{1}{3}, h\right), \left(\frac{1}{3}, \frac{1}{3}, 0\right)\right) \\ &= D\left(\Lambda_{\{\frac{1}{3}, \frac{1}{3}\}}(p, q, h), \Lambda_{\{\frac{1}{3}, \frac{1}{3}\}}(p, q, 0)\right) \\ &\leq D((p, q, h), (p, q, 0)), \end{aligned} \quad (E11)$$

where the final inequality is due to the contractivity of the distance D , whereas the first equality is due to the fact that

$$\left(\frac{1}{3}, \frac{1}{3}, h\right) = \Lambda_{\{\frac{1}{3}, \frac{1}{3}\}}(p, q, h), \quad (E12)$$

which in turn is due to Eqs. (E4), (E5), and:

$$U_1\{c_1, c_2, c_3\}U_1^\dagger = \{-(-1)^{N/2}c_2, -(-1)^{N/2}c_3, c_1\}, \quad (E13)$$

$$U_2\{c_1, c_2, c_3\}U_2^\dagger = \{c_3, -(-1)^{N/2}c_1, -(-1)^{N/2}c_2\}. \quad (E14)$$

In order to prove the opposite inequality and thus Eq. (E7), we now introduce a global N -qubit channel Ω with operator-sum representation

$$\Omega(\varrho) = \sum_{i=1}^{2^N} A_i \varrho A_i^\dagger, \quad (E15)$$

where

$$\begin{aligned} \{A_i\}_{i=1}^{2^N} &= \left\{ \{|\Psi_j^+\rangle\langle\Phi_j^+\rangle\}_{j=1}^{2^{N-2}}, \{|\Psi_j^+\rangle\langle\Phi_j^-\rangle\}_{j=1}^{2^{N-2}}, \right. \\ &\quad \left. \{|\Psi_j^-\rangle\langle\Phi_j^+\rangle\}_{j=1}^{2^{N-2}}, \{|\Psi_j^-\rangle\langle\Phi_j^-\rangle\}_{j=1}^{2^{N-2}} \right\} \end{aligned} \quad (E16)$$

with the 2^N Kraus operators satisfying $\sum_i A_i^\dagger A_i = \mathbb{I}^{\otimes N}$, where $\{|\Phi_j^\pm\rangle\}$ and $\{|\Psi_j^\pm\rangle\}$ constitute the binary ordered N -qubit eigenvectors $\{|\beta_i^\pm\rangle\}$ with even and odd parity, respectively, i.e. they are such that

$$\begin{aligned} \Pi_3|\Phi_j^\pm\rangle &= |\Phi_j^\pm\rangle, \\ \Pi_3|\Psi_j^\pm\rangle &= -|\Psi_j^\pm\rangle, \end{aligned} \quad (E17)$$

where $j \in \{1, \dots, 2^{N-2}\}$. It will be crucial in the following to see that the effect of Ω on an \mathcal{M}_N^3 state represented by the triple $(\frac{1}{3}, \frac{1}{3}, h)$ is given by

$$\Omega\left(\left(\frac{1}{3}, \frac{1}{3}, h\right)\right) = (1, 0, h). \quad (E18)$$

Thanks to Eqs. (B3) and (E17), one gets that the spectral decomposition of an \mathcal{M}_N^3 state with even N can be written as follows:

$$\begin{aligned} & \{c_1, c_2, c_3\} \\ &= \frac{1}{2^N} \left[1 + c_1 + (-1)^{N/2}c_2 + c_3 \right] \sum_j |\Phi_j^+\rangle\langle\Phi_j^+| \\ &\quad + \frac{1}{2^N} \left[1 - c_1 - (-1)^{N/2}c_2 + c_3 \right] \sum_j |\Phi_j^-\rangle\langle\Phi_j^-| \\ &\quad + \frac{1}{2^N} \left[1 + c_1 - (-1)^{N/2}c_2 - c_3 \right] \sum_j |\Psi_j^+\rangle\langle\Psi_j^+| \\ &\quad + \frac{1}{2^N} \left[1 - c_1 + (-1)^{N/2}c_2 - c_3 \right] \sum_j |\Psi_j^-\rangle\langle\Psi_j^-|. \end{aligned} \quad (E19)$$

Consequently, the spectral decompositions of the \mathcal{M}_N^3 states represented by the triples $(\frac{1}{3}, \frac{1}{3}, h)$ and $(1, 0, h)$ are, respec-

tively,

$$\begin{aligned}
\left(\frac{1}{3}, \frac{1}{3}, h\right) &= \left\{ -\frac{2h+1}{3}, (-1)^{N/2} \frac{2h+1}{3}, -\frac{2h+1}{3} \right\} \\
&= \frac{1}{2^{N-1}} \left(\frac{1-h}{3}\right) \sum_j |\Phi_j^+\rangle\langle\Phi_j^+| \\
&\quad + \frac{1}{2^{N-1}} \left(\frac{1-h}{3}\right) \sum_j |\Phi_j^-\rangle\langle\Phi_j^-| \\
&\quad + \frac{1}{2^{N-1}} \left(\frac{1-h}{3}\right) \sum_j |\Psi_j^+\rangle\langle\Psi_j^+| \\
&\quad + \frac{1}{2^{N-1}} (1+h) \sum_j |\Psi_j^-\rangle\langle\Psi_j^-|,
\end{aligned} \tag{E20}$$

and

$$\begin{aligned}
(1, 0, h) &= \left\{ -h, (-1)^{N/2}h, -1 \right\} \\
&= \frac{1}{2^{N-1}} (1-h) \sum_j |\Psi_j^+\rangle\langle\Psi_j^+| \\
&\quad + \frac{1}{2^{N-1}} (1+h) \sum_j |\Psi_j^-\rangle\langle\Psi_j^-|.
\end{aligned} \tag{E21}$$

By exploiting the following equalities

$$\begin{aligned}
\Omega(|\Phi_j^+\rangle\langle\Phi_j^+|) &= |\Psi_j^+\rangle\langle\Psi_j^+|, \\
\Omega(|\Phi_j^-\rangle\langle\Phi_j^-|) &= |\Psi_j^-\rangle\langle\Psi_j^-|, \\
\Omega(|\Psi_j^+\rangle\langle\Psi_j^+|) &= |\Psi_j^+\rangle\langle\Psi_j^+|, \\
\Omega(|\Psi_j^-\rangle\langle\Psi_j^-|) &= |\Psi_j^-\rangle\langle\Psi_j^-|,
\end{aligned} \tag{E22}$$

and the linearity of the channel Ω , we immediately get Eq. (E18). We then have the inequality

$$\begin{aligned}
D((p, q, h), (p, q, 0)) &= D\left(\Lambda_{\{p, q\}}\left(\Omega\left(\frac{1}{3}, \frac{1}{3}, h\right)\right), \Lambda_{\{p, q\}}\left(\Omega\left(\frac{1}{3}, \frac{1}{3}, 0\right)\right)\right) \\
&\leq D\left(\left(\frac{1}{3}, \frac{1}{3}, h\right), \left(\frac{1}{3}, \frac{1}{3}, 0\right)\right),
\end{aligned} \tag{E23}$$

where the final inequality is again due to the contractivity of the distance D , whereas the first equality is due to the fact that

$$(p, q, h) = \Lambda_{\{p, q\}}\left(\Omega\left(\frac{1}{3}, \frac{1}{3}, h\right)\right),$$

which in turn is due to Eqs. (E18), (E8), (E5) and (E4). By putting together the two opposite inequalities (E11) and (E23), we immediately get the invariance of Eq. (E7) for any contractive distance. \blacksquare

Now we are ready to find out the analytical expression of one of the closest $\{K'_\alpha\}_{\alpha=1}^M$ -separable (resp., M' -separable) states ς_ϖ to any \mathcal{M}_N^3 state ϖ belonging to the $\{-1, (-1)^{N/2}, -1\}$ -corner.

Theorem E.1. *For any even N , according to any convex and contractive distance, the \mathcal{M}_N^3 state $(p, q, 0)$ is one of the closest $\{K'_\alpha\}_{\alpha=1}^M$ -separable (resp., M' -separable) states to the \mathcal{M}_N^3 state (p, q, h) .*

Proof.

Thanks to Lemma E.1, which holds for any convex and contractive distance and any even N , we just need to prove that for any $p', q' \in [0, 1]$, $p' + q' \leq 1$,

$$D((p, q, h), (p, q, 0)) \leq D((p, q, h), (p', q', 0)).$$

In fact

$$\begin{aligned}
D((p, q, h), (p, q, 0)) &= D\left(\left(\frac{1}{3}, \frac{1}{3}, h\right), \left(\frac{1}{3}, \frac{1}{3}, 0\right)\right) \\
&= D\left(\Lambda_{\{\frac{1}{3}, \frac{1}{3}\}}(p, q, h), \Lambda_{\{\frac{1}{3}, \frac{1}{3}\}}(p', q', 0)\right) \\
&\leq D((p, q, h), (p', q', 0)),
\end{aligned}$$

where the first equality is due to Lemma E.2, which holds for any contractive distance and any even N , the second equality is due to the fact that

$$\left(\frac{1}{3}, \frac{1}{3}, h\right) = \Lambda_{\{\frac{1}{3}, \frac{1}{3}\}}(p, q, h), \tag{E24}$$

$$\left(\frac{1}{3}, \frac{1}{3}, 0\right) = \Lambda_{\{\frac{1}{3}, \frac{1}{3}\}}(p', q', 0), \tag{E25}$$

with $\Lambda_{\{\frac{1}{3}, \frac{1}{3}\}}$ representing the LOCC expressed by Eq. (E8), and finally the inequality is due to the contractivity of the distance D . \blacksquare

Now that we know the analytical expression of one of the closest $\{K'_\alpha\}_{\alpha=1}^M$ - and M' -separable states to any \mathcal{M}_N^3 state with even N according to any convex and contractive distance, we can unveil the general hierarchy of both the $\{K'_\alpha\}_{\alpha=1}^M$ - and M' -inseparable multiparticle entanglement of these \mathcal{M}_N^3 states with respect to any geometric entanglement monotone $E_{\{K'_\alpha\}_{\alpha=1}^M}^D$ and $E_{M'}^D$, respectively.

Corollary E.1. *For every even N and according to any valid geometric measure of $\{K'_\alpha\}_{\alpha=1}^M$ - and M' -inseparable multiparticle entanglement $E_{\{K'_\alpha\}_{\alpha=1}^M}^D$ and $E_{M'}^D$, the following holds:*

$$E_{\{K'_\alpha\}_{\alpha=1}^M}^D((p, q, h)) = E_{\{K'_\alpha\}_{\alpha=1}^M}^D((p', q', h)) \tag{E26}$$

$$E_{M'}^D((p, q, h)) = E_{M'}^D((p', q', h)) \tag{E27}$$

$$E_{\{K'_\alpha\}_{\alpha=1}^M}^D((p, q, h)) \leq E_{\{K'_\alpha\}_{\alpha=1}^M}^D((p', q', h')), \tag{E28}$$

$$E_{M'}^D((p, q, h)) \leq E_{M'}^D((p', q', h')), \tag{E29}$$

for any $h \leq h'$.

Proof.

Let us start by proving Eq. (E26). By using Theorem E.1 and Lemma E.2, we obtain

$$\begin{aligned} E_{\{K'_\alpha\}_{\alpha=1}^M}^D((p, q, h)) &= D((p, q, h), (p, q, 0)) \\ &= D\left(\left(\frac{1}{3}, \frac{1}{3}, h\right), \left(\frac{1}{3}, \frac{1}{3}, 0\right)\right) \\ &= D((p', q', h), (p', q', 0)) \\ &= E_{\{K'_\alpha\}_{\alpha=1}^M}^D((p', q', h)), \end{aligned} \quad (\text{E30})$$

for any $p, q, p', q' \in [0, 1]$, $p+q \leq 1$, $p'+q' \leq 1$ and $h \in [0, 1]$.

In order to prove Eq. (E28), let us consider the \mathcal{M}_N^3 states $\varpi = (p, q, h)$, $\varpi' = (p, q, h')$ such that $h \leq h'$, and $\varsigma = \varsigma_\varpi = \varsigma_{\varpi'} = (p, q, 0)$, which is one of the closest $\{K'_\alpha\}_{\alpha=1}^M$ -separable states to both ϖ and ϖ' according to Theorem E.1. We can write $\varpi = \lambda\varpi' + (1 - \lambda)\varsigma$, for some $\lambda \in [0, 1]$. Now, by using the convexity of the distance and Eq. (E26), we get

$$\begin{aligned} E_{\{K'_\alpha\}_{\alpha=1}^M}^D((p, q, h)) &= D(\varpi, \varsigma) \\ &= D(\lambda\varpi' + (1 - \lambda)\varsigma, \varsigma) \\ &\leq \lambda D(\varpi', \varsigma) + (1 - \lambda)D(\varsigma, \varsigma) \\ &= \lambda D(\varpi', \varsigma) \\ &\leq D(\varpi', \varsigma) \\ &= E_{\{K'_\alpha\}_{\alpha=1}^M}^D((p, q, h')) \\ &= E_{\{K'_\alpha\}_{\alpha=1}^M}^D((p', q', h')). \end{aligned} \quad (\text{E31})$$

In order to prove Eqs. (E27) and (E29), we just remark that exactly the same proof holds when substituting $\{K'_\alpha\}_{\alpha=1}^M$ -separability with M' -separability.

$(\sum_i \sqrt{p_i q_i})^2$ is the classical fidelity. Consequently, by using Eq. (E20) to get both P_h and P_0 , we obtain the desired expressions for $f_D(h)$.

2. Odd N case

Let us now turn our attention to the evaluation of the geometric multiparticle entanglement $E_{\{K'_\alpha\}_{\alpha=1}^M}^D(\varpi)$ and $E_{M'}^D(\varpi)$ of an \mathcal{M}_N^3 state ϖ in the case of odd N . Unlike the even N case, where all the convex and contractive distances D concur on what is one of the closest separable states to an \mathcal{M}_N^3 state, there is unfortunately no such agreement in the odd N case. In the following we will focus in particular on the trace distance-based geometric measures of multiparticle entanglement $E_{\{K'_\alpha\}_{\alpha=1}^M}^{D_{\text{Tr}}}(\varpi)$ and $E_{M'}^{D_{\text{Tr}}}(\varpi)$ of any \mathcal{M}_N^3 state with odd N , when considering as usual a partition $\{K'_\alpha\}_{\alpha=1}^M$ such that K'_α is odd for more than one value of α and a number of parties $M' > \lceil N/2 \rceil$, respectively.

We know that the trace distance-based multiparticle entanglement of an \mathcal{M}_N^3 state ϖ with odd N is the minimal distance from ϖ to the unit octahedron O_1 . Due to convexity of the trace distance and of the unit octahedron O_1 , we get that one of the closest $\{K'_\alpha\}_{\alpha=1}^M$ -separable (resp., M' -separable) \mathcal{M}_N^3 states to an entangled \mathcal{M}_N^3 state ϖ must belong necessarily to the boundary of the octahedron, i.e. either to one of its faces or edges. We can easily see that the trace distance between two arbitrary odd N \mathcal{M}_N^3 states $\varpi_1 = \{c_1^{(1)}, c_2^{(1)}, c_3^{(1)}\}$ and $\varpi_2 = \{c_1^{(2)}, c_2^{(2)}, c_3^{(2)}\}$ is nothing but one half of the Euclidean distance between their representing triples, i.e.

$$D_{\text{Tr}}(\varpi_1, \varpi_2) = \frac{1}{2} \sqrt{\sum_{i=1}^3 (c_i^{(1)} - c_i^{(2)})^2}. \quad (\text{E32})$$

This is proven as follows. In order to evaluate the trace distance between any two \mathcal{M}_N^3 states with odd N , we just need to calculate the eigenvalues of their difference, because

$$D_{\text{Tr}}(\varpi_1, \varpi_2) = \frac{1}{2} \text{Tr}(|\varpi_1 - \varpi_2|) = \frac{1}{2} \sum_i |\lambda_i|, \quad (\text{E33})$$

where $\{\lambda_i\}$ are just the eigenvalues of $\varpi_1 - \varpi_2$. Since $\varpi_1 - \varpi_2 = \frac{1}{2^N} \sum_i d_i \sigma_i^{\otimes N}$, with $d_i = c_i^{(1)} - c_i^{(2)}$, one can easily see that its eigenvectors are exactly the ones expressed in Eq. (B5), with $d_1 = r \sin \theta \cos \phi$, $d_2 = r \sin \theta \sin \phi$ and $d_3 = r \cos \theta$ while its eigenvalues are given by either $\frac{1}{2^N} r$ or $-\frac{1}{2^N} r$, with $r = \sqrt{d_1^2 + d_2^2 + d_3^2}$. By putting these eigenvalues into Eq. (E33) one immediately gets Eq. (E32).

An immediate consequence of Eq. (E32) is that the closest $\{K'_\alpha\}_{\alpha=1}^M$ -separable (resp., M' -separable) \mathcal{M}_N^3 state $\varsigma_\varpi = \{s_1, s_2, s_3\}$ to an entangled \mathcal{M}_N^3 state $\varpi = \{c_1, c_2, c_3\}$ is just its Euclidean orthogonal projection onto the boundary of the unit octahedron O_1 . We can thus distinguish between the following two cases:

We are now ready to apply the above general results to calculate the geometric multiparticle entanglement $E_{\{K'_\alpha\}_{\alpha=1}^M}^D(\varpi)$ and $E_{M'}^D(\varpi)$ of any \mathcal{M}_N^3 state ϖ for particular instances of D . As we have just shown, for \mathcal{M}_N^3 states in the $\{-1, (-1)^{N/2}, -1\}$ -corner, $E_{\{K'_\alpha\}_{\alpha=1}^M}^D(\varpi) = E_{M'}^D(\varpi) = D\left(\left(\frac{1}{3}, \frac{1}{3}, h\right), \left(\frac{1}{3}, \frac{1}{3}, 0\right)\right) = f_D(h)$, where $f_D(h)$ is some monotonically increasing function of h only, which depends on the chosen distance D . By local unitary equivalence, this is true indeed for any \mathcal{M}_N^3 state in any of the four corners if we define the generalised h to be $h_\varpi = \frac{1}{2}(\sum_{j=1}^3 |c_j| - 1)$. Table I in the main text shows $f_D(h_\varpi)$ for the relative entropy, trace, infidelity, squared Bures, and squared Hellinger distance.

Here we show the derivation of the given expressions for $f_D(h)$. Since the two \mathcal{M}_N^3 states $\left(\frac{1}{3}, \frac{1}{3}, h\right)$ and $\left(\frac{1}{3}, \frac{1}{3}, 0\right)$ are diagonal in the same basis, we have that their distance reduces to the corresponding classical distance between the probability distributions formed by their eigenvalues, denoted by P_h and P_0 respectively. We recall that the classical relative entropy, trace, infidelity, squared Bures, and squared Hellinger distance between two probability distributions $P = \{p_i\}$ and $Q = \{q_i\}$ are given by, respectively $D_{\text{RE}}(P, Q) = \sum_i p_i \log_2(p_i/q_i)$, $D_{\text{Tr}}(P, Q) = \sum_i |p_i - q_i|/2$, $D_{\text{F}}(P, Q) = 1 - F(P, Q)$, and $D_{\text{B}}(P, Q) = D_{\text{H}}(P, Q) = 2(1 - \sqrt{F(P, Q)})$, where $F(P, Q) =$

1. the Euclidean projection of $\{c_1, c_2, c_3\}$ onto the boundary of the unit octahedron O_1 falls onto one of its faces. This case happens if, and only if, $0 \leq \text{sign}(c_i)s_i \leq 1$ for any i , where $\{s_i = \text{sign}(c_i)(1 - |c_1| - |c_2| - |c_3| + 3|c_i|)/3\}$ is exactly the triple representing such Euclidean projection;
2. the Euclidean projection of $\{c_1, c_2, c_3\}$ onto the boundary of the unit octahedron O_1 falls onto one of its edges. This case happens when any of the conditions listed in case 1 do not hold. Moreover, the triple $\{s_1, s_2, s_3\}$ representing such Euclidean projection is given by $s_k = 0$ and $s_i = \text{sign}(c_i)(1 - \sum_{j \neq k} |c_j| + 2|c_i|)/2$, where k is set by $f_k = \min\{f_1, f_2, f_3\}$ with $f_i = \sqrt{c_i^2 + (1 - \sum_{j \neq i} |c_j|)^2}/2$.

This provides the explicit expression reported in Eq. (3) in the main text.

Appendix F: Genuine geometric multiparticle entanglement of the GHZ-diagonal states

In this appendix we will adopt our approach to evaluate exactly the geometric genuine multiparticle entanglement E_2^D of any N -qubit GHZ-diagonal state ξ with respect to any contractive and jointly convex distance D .

Recall that any N -qubit state ϱ can be transformed via a single-qubit LOCC Γ into a GHZ-diagonal state $\varrho_{\text{GHZ}} \equiv \Gamma(\varrho)$ with eigenvalues given by $p_i^\pm = \langle \beta_i^\pm | \varrho | \beta_i^\pm \rangle$ [21], a procedure referred to as GHZ-diagonalisation of ϱ in the main text. The entanglement quantification is then based on the following two arguments.

First, we have that one of the closest 2-separable states to a GHZ-diagonal state is itself GHZ-diagonal. Indeed, for any GHZ-diagonal state ξ and any 2-separable state ς , we have that

$$D(\xi, \varsigma_{\text{GHZ}}) = D(\Gamma(\xi), \Gamma(\varsigma)) \leq D(\xi, \varsigma), \quad (\text{F1})$$

where in the first equality we use the invariance of any GHZ-diagonal state through Γ and that $\Gamma(\varsigma) \equiv \varsigma_{\text{GHZ}}$ is the GHZ-diagonalisation of ς , and in the inequality we use the contractivity of the distance through any completely positive trace-preserving channel. Moreover, the GHZ-diagonalisation ς_{GHZ} of any 2-separable state ς is a 2-separable GHZ-diagonal state since Γ is a single-qubit LOCC.

Therefore, the set \mathcal{S}_2^G of 2-separable GHZ-diagonal states turns out to be the relevant one in order to compute exactly any distance-based measure of genuine multiparticle entanglement of a GHZ-diagonal state ξ , thus dramatically simplifying the ensuing optimisation as follows:

$$E_2^D(\xi) \equiv \inf_{\varsigma \in \mathcal{S}_2} D(\xi, \varsigma) = \inf_{\varsigma_{\text{GHZ}} \in \mathcal{S}_2^G} D(\xi, \varsigma_{\text{GHZ}}). \quad (\text{F2})$$

Now, let us consider an arbitrary GHZ-diagonal state ξ and rearrange its GHZ eigenstates $\{|\beta_i\rangle\}_{i=1}^{2^N}$ in such a way that the corresponding eigenvalues $\{p_i^\xi\}_{i=1}^{2^N}$ are in non-increasing order. It is well known that ξ is 2-separable if, and only if, $p_1^\xi \leq 1/2$ [11]. For $p_1^\xi > 1/2$, we will show that one of the closest 2-separable GHZ-diagonal states ς_ξ has eigenvalues $\{p_i^{\varsigma_\xi}\}_{i=1}^{2^N}$ such that $p_1^{\varsigma_\xi} = 1/2$, with $\{p_i^{\varsigma_\xi}\}_{i=1}^{2^N}$ corresponding again to the ordering of GHZ eigenstates $\{|\beta_i\rangle\}_{i=1}^{2^N}$ set by ξ . This result further simplifies the optimisation in Eq. F2.

Consider any 2-separable GHZ-diagonal state ς , it holds that there will always be a 2-separable GHZ-diagonal state ς' with eigenvalues $\{p_i^{\varsigma'}\}_{i=1}^{2^N}$ and $p_1^{\varsigma'} = 1/2$ such that $\varsigma' = \lambda\xi + (1 - \lambda)\varsigma$ for some $\lambda \in [0, 1]$. Now, for any convex distance, the following holds

$$\begin{aligned} & D(\xi, \varsigma') \\ &= D(\xi, \lambda\xi + (1 - \lambda)\varsigma) \\ &\leq \lambda D(\xi, \xi) + (1 - \lambda)D(\xi, \varsigma) \\ &= (1 - \lambda)D(\xi, \varsigma) \\ &\leq D(\xi, \varsigma). \end{aligned} \quad (\text{F3})$$

This inequality immediately implies that one of the closest 2-separable GHZ-diagonal states ς_ξ to a 2-inseparable GHZ-diagonal state ξ is of the form ς' , which is formalised as a corollary below.

Corollary F.1. *For any convex and contractive distance D and any fully inseparable GHZ-diagonal state ξ , whose GHZ eigenstates $\{|\beta_i\rangle\}_{i=1}^{2^N}$ are arranged such that the corresponding eigenvalues $\{p_i^\xi\}_{i=1}^{2^N}$ are in non-increasing order, one of the closest 2-separable states ς_ξ to ξ is itself a GHZ-diagonal state with eigenvalues $\{p_i^{\varsigma_\xi}\}_{i=1}^{2^N}$ such that $p_1^{\varsigma_\xi} = 1/2$, with $\{p_i^{\varsigma_\xi}\}_{i=1}^{2^N}$ corresponding again to the ordering of GHZ eigenstates $\{|\beta_i\rangle\}_{i=1}^{2^N}$ set by ξ .*

We can now apply this Corollary to calculate the geometric genuine multiparticle entanglement $E_2^D(\xi)$ of any GHZ-diagonal state ξ for particular instances of D . Since the closest 2-separable state ς_ξ to a GHZ-diagonal state ξ is also a GHZ-diagonal state, they are diagonal in the same basis and their distance reduces to the corresponding classical distance between the probability distributions formed by their eigenvalues, denoted by P_ξ and P_{ς_ξ} respectively. By using the expressions given earlier in Appendix E of the classical relative entropy, trace, infidelity, squared Bures, and squared Hellinger distance between two probability distributions P_ξ and P_{ς_ξ} , and minimising it over all probability distributions P_{ς_ξ} such that $p_1^{\varsigma_\xi} = 1/2$, one easily obtains the desired expressions for $E_2^D(\xi)$ expressed in the main text.